PlankTOM10 User Manual
Version 1.02

Clare Enright, Erik Buitenhuis, Meike Vogt and Corinne Le Quéré

March 25, 2009

Contents

Chapter 1

The Plankton Type Ocean Model (PlankTOM) Series

The ocean biogeochemical general circulation model, PlankTOM, consists of three coupled sub-models, describing

- the circulation and ocean physics (Ocean General Circulation model)
- the interaction of the ocean with the sea-ice (Sea-Ice Model).
- the marine ecosystem and its interactions with physics and chemistry and the cycling of elements between ocean and atmosphere (Ocean biogeochemistry model)

This manual fully describes the biogeochemistry model, with detailed descriptions of each of the model tracers included in current versions. The ocean circulation and sea-ice model are only described in brief, as literature regarding these models is available elsewhere, see http://www.nemo-ocean.eu.

1.1 Introduction

The ocean biogeochemistry model simulates the oceanic cycling of the basic chemical constituents of "System Earth" in the marine domain, such as the carbon and nitrogen cycles. Biological, physical, chemical and geological processes contribute to the sources and sinks of nutrients (e.g. phosphate) and gases (e.g. oxygen). We use Dynamic Green Ocean Models (DGOMs) that put a particular emphasis on simulating the biological components of marine ecosystems, as biological feedbacks are among the least understood in the climate system (IPCC, 2007). In particular and with respect to recent anthropogenic climate change, these feedbacks are of major interest to the scientific community.

1.1.1 PlankTOM history

Maier-Reimer (1993) described the model HAMOCC3 in which the effect of the biological pump on carbon distribution was included in the Hamburg model of ocean circulation. Further development resulted in the PISCES model of Aumont et al. (2003) which includes two phytoplankton groups and two zooplankton size classes. The PlankTOM series of models were developed from the PISCES-T ocean biogeochemistry model which represents ecosystem dynamics based on Plankton Functional Types (PFTs; Le Quéré et al., 2005). All operational models of the PlankTOM series are Dynamic Green Ocean Models (DGOMs) and contain the full biogeochemical cycles of phosphate, silicate, carbon, oxygen and a simplified iron cycle (Aumont et al., 2003). Currently, within the framework of the Dynamic Green Ocean Project, a fully functional 10 PFT model is being developed (PlankTOM10, Le Quéré et al., 2005). Represented PFTs contain groups of organisms carrying out a well-defined biogeochemical function in the marine environment, such as calcification, nitrogen fixation or DMS production, for example. Due to this definition, a PFT may contain a spectrum of genetically diverse organisms. For example, the silicifiers contain all types of diatoms (both chain-forming and individual cells). However, due to the scarcity of laboratory data, the initial parametrisation of a PFT is often based on data of one single or only few "model species". Data on

calcifiers, for example, are dominated by the well-studied and easy-to-culture coccolithophore *Emiliania huxleyi*, even though many other, more abundant species exist in this group. However, several experimental projects have now embarked on studying the characteristics of a wider spectrum of organisms for most of the PFTs, i.e. coccolithophores (Buitenhuis et al., 2008), diatoms (Sarthou et al., 2005), different size classes of heterotrophs (Moriarty, in prep.) The results from these studies will allow a better representation of a PFT for a whole spectrum of often taxonomically different groups, as shown by Buitenhuis et al., 2006a. Where the results do not fully define the ecological niche of the PFT, the initial parameters obtained from the literature are then tuned within the range of observational uncertainty for the group of organisms to be represented, to secure survival of the PFT. In order to represent bulk properties such as total chlorophyll and primary production or species distribution as detected from satellites (SeaWiFS), underconstrained parameters that define PFT interactions are tuned, in particular food preferences of zooplankton]. All versions of PlankTOM are global models with one global set of parameters, but they can also be used for local and regional applications. Prognostic variables are the three dimensional tracer concentrations. The serial number designates the number of explicitly represented PFTs in the model.

1.2 Criteria for selection of a PFT

Le Quéré et al. (2005) argued that a PFT should be explicitly modelled when:

- a group of plankton taxa has an explicit biogeochemical role in the ocean
- a group is defined by a distinct set of physiological, environmental, or nutrient requirements, which define its biomass and productivity
- the behaviour of a group has distinct effects on the performance of other PFTs, for instance through selective depletion of nutrients or grazing, and
- the group is of quantitative importance in at least some regions of the ocean.

As a result Le Quéré et al. (2005) identified a set of 10 key PFT (summarised in Table 1) and undertook the construction of a global Dynamic Green Ocean Model (DGOM) based on these PFT, to be used for the study of ecosystem-climate interactions (Figure 1.1).

1.3 Autotrophs and their functional role in the ocean

1.3.1 Pico-autotrophs - PIC

Pico-autotrophs (picoeukaryotes and non N_2-fixing photosynthetic bacteria such as Synechococcus and Prochlorococcus) make a substantial contribution to primary production, but a negligible contribution to export. They have high affinities for nutrients and light due to their high surface to volume ratio. They are found everywhere and constitute an important fraction of phytoplankton biomass in High Nutrient Low Chlorophyll (HNLC) and oligotrophic regions.

1.3.2 N_2-fixers - FIX

Phytoplankton N_2-fixers (e.g. Trichodesmium and N_2-fixing unicellular procaryotes) can use N_2 from the atmosphere and thus control the total ocean inventory of reactive N. N_2-fixation requires more energy than the acquisition of other dissolved organic or inorganic nitrogen form. It is inefficient at low temperatures. Thus N_2-fixers are advantaged in warm nutrient-poor waters, but out-competed elsewhere. Although the true Fe demand of these organisms is not firmly established, it has been suggested that aeolian Fe input may play an indirect role in determining fixation by the phytoplankton and total ocean new production over millennial time scales. The requirement of N_2-fixers for P is also the basis for a proposed mechanism by which P supply tightly regulates the oceanic N inventory .

1.3.3 Calcifiers - COC

Phytoplankton calcifiers (e.g. coccolithophores) produce more than half of the marine carbonate flux and thereby influence atmospheric CO_2 on millennial time scales through the effect of calcification on ocean alkalinity. Phytoplankton calcifiers also produce the densest ballast observed in sinking particles. They have the ability to use organic P but they die after one day in the dark, which suggests that they would be penalized in regions where the mixing depth of the ocean is below the euphotic zone. The feedbacks between calcification and atmospheric CO_2 concentration (low pH) is different for two different species of coccolithophores, and the role of low Zn concentrations has not been firmly established.

1.3.4 DMSp producers - PHA

Phytoplankton DMSp-producers (e.g. Phaeocystis and small ($<$20 μm) autotrophic flagellates) produce dimethylsulfoniopropionate (DMSP) and convert it to DMS using an extracellular enzyme (DMSP-lyase). Thus they affect the atmospheric sulphur cycle. Other nano- and pico- plankton also produce DMSP. DMS-producers have a high requirement for P. They are particularly abundant in coastal areas, where, under certain environmental condirtions, they are often observed in colonies. Calcifiers are also important for the DMS cycle but they are treated independently.

1.3.5 Mixed phytoplankton - MIX

Mixed-phytoplankton (e.g. autotrophic dinoflagellates and Chrysophyceae) represent phytoplankton of heterogenic size (2-200 μm) and taxonomic composition for which no distinct biogeochemical role is defined. This PFT constitutes the background biomass of blooming which do not bloom in the open ocean, have low seasonality, and no direct impact on the cycles of S, Si or $CaCO_3$.

1.3.6 Silicifiers - DIA

Phytoplankton silicifiers (e.g. diatoms) dominate micro-phytoplankton (20-200 μm) assemblages and contribute most of the primary production and biomass during the spring bloom in temperate and polar regions. Silicifiers contribute to carbon export far more effectively than smaller plankton through direct sinking of single cells, key grazing pathways, and through mass sedimentation events at the end of the spring blooms when nutrients are depleted. Silicifiers require and deplete Si. They require Si and more Fe and P than most of the smaller nano and pico phytoplankton. They respond to enhanced Fe input in HNLC regions as long as Si remains available. They produce little DMSP compared to some other phytoplankton.

1.4 Heterotrophs and their functional role in the ocean

1.4.1 Proto-zooplankton - PRO

Proto-zooplankton (e.g. ciliates, heterotrophic flagellates) are unicellular heterotrophs (5-200 μm) which dampen bloom formation of small phytoplankton. They graze preferentially on small phytoplankton (1-20 μm), such as the pico- and nano-phytoplankton PFTs. Their growth rates are similar to that of phytoplankton in the pico and nano size range, and their ingestion rates are coupled to the production rates of their prey.

1.4.2 Meso-zooplankton - MES

Meso-zooplankton (e.g. copepods, euphausiids) produce large and fast-sinking faecal pellets and are an important source of food for fishes. They graze preferentially on larger plankton (20 to 200 μm), such as proto-zooplankton and phytoplankton silicifiers. Their grazing and reproductive rates are slower than that of proto-zooplankton.

1.4.3 Macro-zooplankton - MAC

Macro-zooplankton (e.g. euphausids, salps, pteropods) also produce large faecal pellets which sink much faster than those of meso-zooplankton. Furthermore, macro-zooplankton graze across a wide spectrum of

sizes (filter feeding) including the smallest phytoplankton, thus their fecal pellets provide an indirect route by which even small phytoplankton biomass can be transferred to the deep ocean. They can achieve very high biomass locally, but they tend to have a patchy distribution. The environmental conditions which control their standing stocks, physiology and life cycles are poorly documented. Meso- and macro-zooplankton such as foraminifera and pteropods also produce $CaCO_3$ and are thought to contribute up to half of the marine carbonate flux.

1.4.4 Pico-heterotrophs BAC

Pico-heterotrophs (heterotrophic bacteria and archaea) remineralise dissolved and particulate organic matter. Remineralisation prevents the export of organic matter to the deep ocean because it converts organic matter to its inorganic form, and releases CO_2 which can be out-gassed back to the atmosphere. They grow rapidly compared to other PFTs.

Table 1: The 10 PFT as suggested by Le Quéré et al. (2005) and their main characteristics.

PFT		Function & characterisation
Pico heterotrophs	BAC	- remineralise dissolved and particulate organic matter
Pico-autotrophs	PIC	- make a substantial contribution to primary production - high affinity for nutrient and light - are ubiquitous - comprise a considerable fraction of biomass in HNLC regions
Phytoplankton N_2-fixers	FIX	- use N_2 from the atmosphere and - control ocean inventory of N - occur in warm, nutrient poor waters
Phytoplankton calcifiers	COC	- produce more than half the marine carbonate flux - influence atmospheric CO_2 on millennium timescales through the effect of calcification on ocean alkalinity - produce the densest ballast - have high light requirements
Phytoplankton DMSp-producers	PHA	- produce dimethylsulphoniopropionate and or dimethylsulphide - affect the global sulphur cycle - have high requirements for phosphorus - abundant in coastal oceans and the Southern Ocean
Mixed phytoplankton	MIX	- are heterogeneous in size and taxonomy - have no distinct biogeochemical role - constitute background biomass (no blooms, low seasonality)
Phytoplankton silicifiers	DIA	- contribute most to primary production and export during spring blooms in temperate and polar regions - contribute effectively to export - require and deplete Si - require more Fe and P than other PFT, but have high maximal growth rate
Proto-zooplankton	PRO	- unicellular heterotrophs - control bloom formation of small phytoplankton - growth similar to phytoplankton - ingestion rates closely coupled to prey production
Meso-zooplankton	PRO	- produce large sinking fecal pellets - are important food source for fishes - graze on larger plankton and proto-zooplankton - slower growth rates than proto-zooplankton
Macro-zooplankton	MAC	- produce large fecal pellets - graze across a wide size spectrum - can be locally abundant, but have patchy distribution - some macro-zooplankton produce $CaCO_3$ and are thought to contribute $1/2$ of the marine carbonate flux

Chapter 2

PlankTOM - Description

2.1 PlankTOM10

PlankTOM10.0 represents 10 PFTs, six phytoplankton functional types (pPFT; pico-phytoplankton, nitrogen fixers, calcifiers, DMS producers, mixed phytoplankton and silicifiers) and four heterotrophic plankton functional types (zPFT; proto-, meso- and macro-zooplankton and pico-heterotrophs). PlankTOM10.0 results from subsequent development of PISCES (Aumont et al., 2003) and, as well as the additional PFTs, includes modifications by Erik Buitenhuis to the meso-zooplankton processes (PISCES-T, Buitenhuis et al., 2006a) and addition of the temperature-dependance of particle remineralisation. Also represented is the ballast effect of sinking particles, based on Stokes' Law and an improved representation of proto-zooplankton rates.

The prognostic variables for the pPFTs are the total PFT biomass, iron, chlorophyll and silicate content. For the three size classes of zPFTs, only the biomass is modeled. All PFTs are assumed to have a constant C/N/P/O ratio. The ratios of Fe/C and Chl/C are variable and fully determined by the model for the phytoplankton. Si/C is determined for diatoms only. In this model, phytoplankton growth is limited by the macronutrients phosphate and nitrate, silicate, iron and light. Phytoplanktonic growth is modelled as the minimum of the potential growth rates on the required nutrients. In addition, the model includes a light penalty scheme, where algae experience higher mortality under low light conditions. Zooplankton feed on phytoplankton, smaller zooplankton and organic matter, with different food preference for each food source.

The modelled nutrients are a phosphate, nitrate, silicate and iron. Phosphate, nitrate and ammonium are not independent but fixed by a constant Redfield ratio. The phosphate/nitrogen pool also undergoes implicit nitrogen fixation and denitrification type processes. In addition to the nutrients, the model also describes 3 further dissolved compartments: dissolved inorganic carbon (DIC), dissolved oxygen (OXY) and alkalinity (ALK). DIC is never limiting. Dissolved oxygen can be used to distinguish oceanic regions with oxic/anoxic remineralization.
Furthermore, there are 7 non-living/detrital compartments: semi-labile dissolved organic matter (DOM), small and large particulate organic matter (POM_s and POM_l), $CaCO_3$ and particulate SiO_2 and the iron content of POM. Small and big particles have variable Fe/C ratios. DOM does not contain any iron. Non-living $CaCO_3$ is released by calcifiers, non living SiO_2 from diatoms.
The inclusion of the ballast effect guarantees refractory sinking of the different tracers: $CaCO_3$ and SiO_2 sink at the same speed as large POM particles, small particles have a fixed sinking speed in $(\frac{m}{d})$. In addition, small and big sinking particles experience aggregation due to turbulence and differential settling. All in all, PlankTOM10 currently comprises of 39 biogeochemical tracers (Table 2).

Figure 1 shows both the included PFTs and their food-web dynamics.

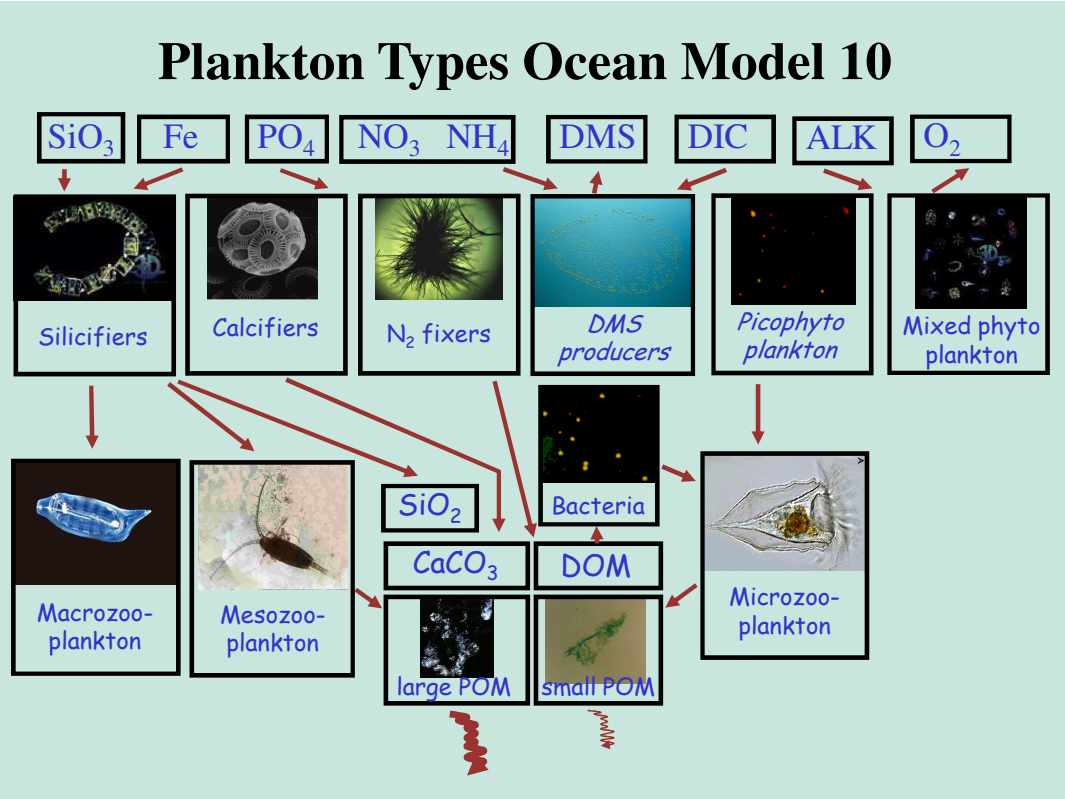

Figure 1: Food-web of PlankTOM10.0. The nutrients iron (Fe), silicate (Si), phosphate (PO_4^-), nitrate (NO_3^-) and ammonia (NH_4^+) are taken up by the 6 pPFTs. The pPFTs (silicifiers (diatoms), calcifiers (coccolithophores), N_2 fixers, DMSP-producers, picophytoplankton and other mixed phytoplankton)) are grazed by the 3 zPFTs: macro-, meso-zooplankton and proto-zooplankton. The silicifiers produce particulate SiO_2, and the calcifiers produce particulate $CaCO_3$, both of which increase the sinking rate of large POC (the ballasting effect. All pPFTs and zPFTs produce dissolved organic matter (DOM), which is degraded by bacteria.

Table 2: List of biogeochemical Tracers in PlankTOM10

Abbreviation	Description	Units
13C*	dissolved inorganic ^{13}C	
ALK	alkalinity	eq L^{-1}
BAC	pico-heterotrophs	mol L^{-1}
BFE	Fe in large POM	
BSI	biogenic particulate silica	mol L^{-1}
CAL	sinking $CaCO_3$	mol L^{-1}
CCH	chlorophyll in calcifiers	mg m^{-3}
CFE	Fe in calcifiers	mol L^{-1}
COC	calcifying phytoplankton	mol L^{-1}
DCH	chlorophyll in silicifiers	mg m^{-3}
DFE	Fe in silicifiers	mol L^{-1}
DIA	silicifying phytoplankton	mol L^{-1}
DIN	dissolved inorganic nitrogeen	mol L^{-1}
DIC	dissolved inorganic carbon	mol L^{-1}
DOC	dissolved organic carbon	mol L^{-1}
DSI	sinking particulate silica	mol L^{-1}
FER	dissolved iron	mol L^{-1}
FCH	chlorophyll in N_2 fixers	mg m^{-3}
FFE	Fe in N_2 fixers	mol L^{-1}
FIX	N_2 fixing phytoplankton	mol L^{-1}
GOC	large particulate organic carbon	mol L^{-1}
HCH	chlorophyll in DMSP producers	mol L^{-1}
HFE	Fe in DMSP producers	mol L^{-1}
PIC	pico-phytoplankton	mol L^{-1}
MES	meso-zooplankton	mol L^{-1}
MIX	mixed phytoplankton	mol L^{-1}
NCH	chlorophyll in mixed phytoplankton	mg m^{-3}
NFE	Fe in mixed phytoplankton	mol L^{-1}
O18*	dissolved ^{18}Oxygen	mol L^{-1}
OXY	dissolved oxygen	mol L^{-1}
PCH	chlorophyll in pico-phytoplankton	mg m^{-3}
PFE	Fe in pico-phytoplankton	mol L^{-1}
PIC	pico-phytoplankton	mol L^{-1}
PHA	DMSp producing phytoplankton	mol L^{-1}
PO4	generic macronutrient	mol L^{-1}
POC	small particulate organic carbon	mol L^{-1}
PRO	proto-zooplankton	mol L^{-1}
SFE	Fe in small POM	mol L^{-1}
SIL	dissolved SiO_3	mol L^{-1}

* Tracers optional.

2.2 3D Tracer description

2.2.1 Notation

In the following chapters, we will show the equations governing tracer and food-web dynamics. These equations are mostly semi-empirical, and have been developed and tested using a multitude of laboratory and field data. As long as not otherwise indicated, both tracers and their respective concentrations will be designated by capital letters, with

- P_i: concentration of pPFT$_i$ with $i \in \{1, 6\}$, (see below for PlankTOM5 note)
- Z_j: concentration of zPFT$_j$, with $j \in \{1, 3\}$, (see below)
- F_k: concentration of food k; where F_k includes phytoplankton and other food sources
- PRO: proto-zooplankton concentration,
- MES: meso-zooplankton concentration,
- MAC: macro-zooplankton concentration,
- PO_4: concentration of phosphate,
- NO_3: concentration of nitrate,
- Fe: iron concentration, and
- Si: silicate concentration.

All concentrations are calculated in ($\frac{mol}{L}$).

Tables are provided which link the mathematical symbols with the variable names used in the Fortran code. All occurrences of variable names and file names (e.g. *namelist.trc.sms*) are indexed. Mathematical symbols are only indexed at the point where they appear as entries in the tables.

Where subscript j includes pico-heterotrophs in additon to the three zoo-plankton types this is stated explicitly.

PlankTOM5 included 3 phytoplankton types (subscript $i \in \{1, 3\}$ and proto- and meso-zooplankton $j \in \{1, 2\}$. Other explicit differences in PlankTOM5 are documented in boxed text.

The ten plankton functional types and the tracers are shown in Figure 2.Figures of this type showing the processes governing the evolution of the PFTs and tracers are included in the follwoing chapters.

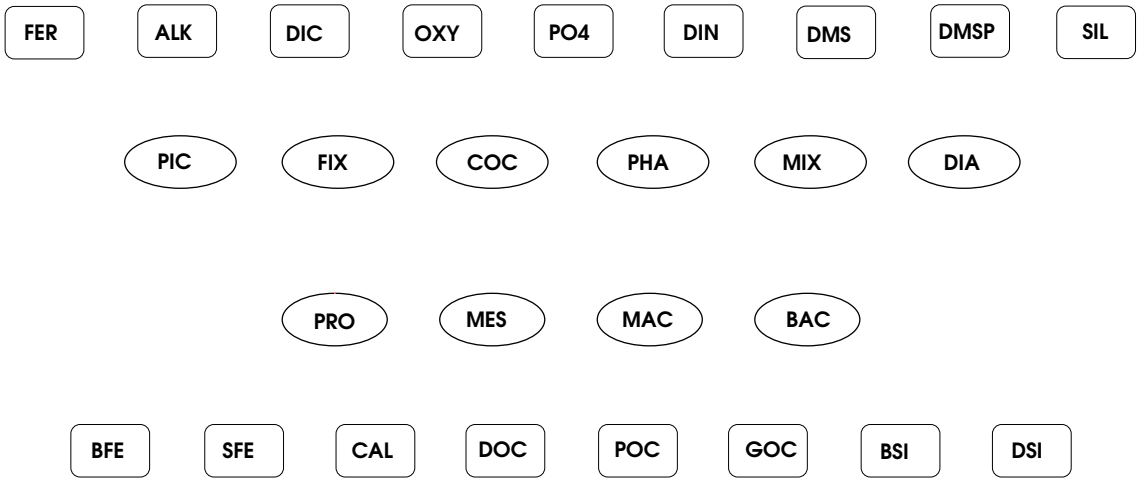

Figure 2: The constituents of PlanktOM10; PFTs are shown as ellipses and tracers as rounded rectangles.Ther are also tracers for the chlorophyll and iron content of the individaul pPFTs but these have been omitted from the figures for clarity.

2.2.2 Tracer Transport

The temporal evolution of all passive tracers T is governed by the balance between its local sources and sinks ('Sources-Minus-Sinks' (SMS), biogeochemical part) and by the physical transport processes (advection and diffusion), hence

$$\frac{dT}{dt} = \nabla \cdot (\vec{u}T) + \nabla \cdot (\vec{K}\nabla T) + SMS, \tag{1}$$

where $\vec{K}$ is the 3-dimensional tracer diffusion coefficient and $\vec{u}$ is the fluid velocity, calculated in the physical model.

Chapter 3

Autotrophic PFTs

3.1 Phytoplankton Biomass - PIC, FIX, COC, PHA, MIX, DIA

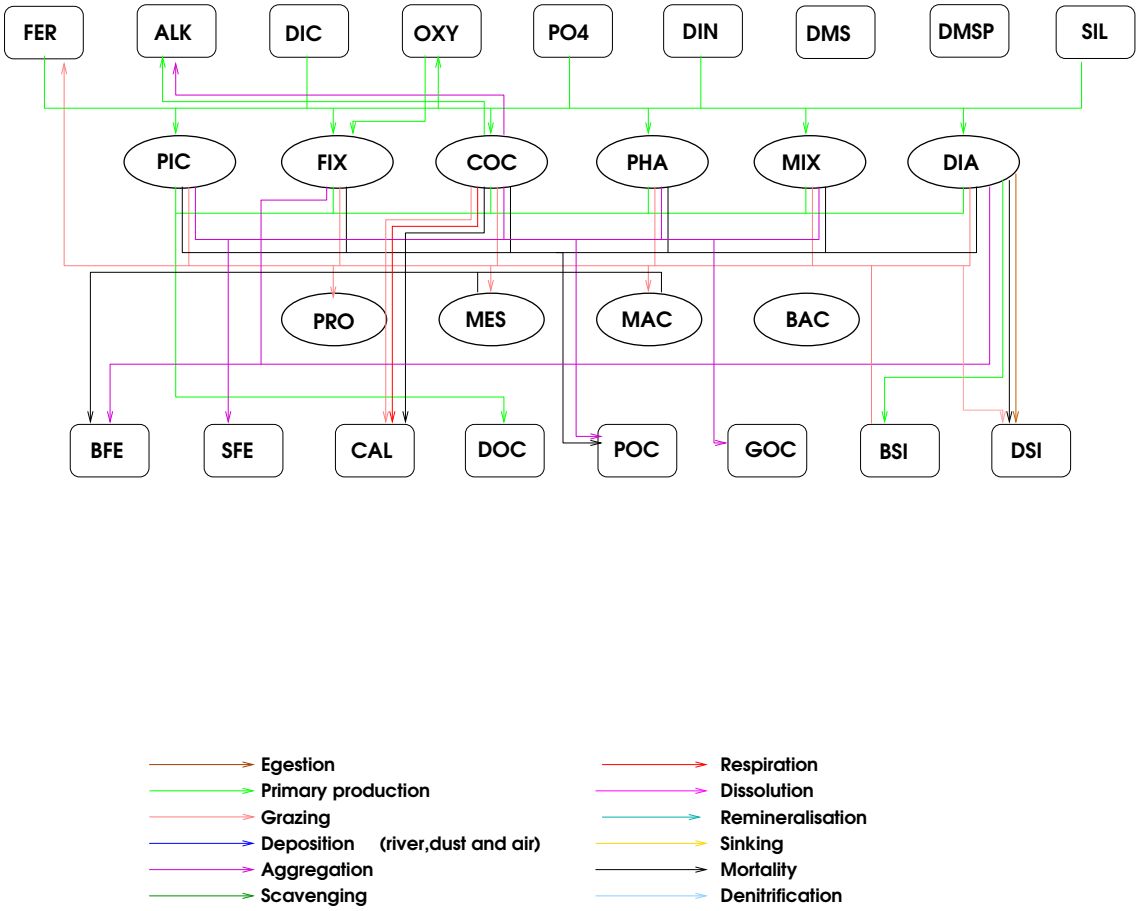

Figure 3: The processes governing the development of the phytoplankton.

The temporal evolution of phytoplankton biomass for each P_i (expressed in terms of carbon, chlorophyll

or iron) is shown in Figure 3 and given in the equation below:

$$\begin{aligned}\frac{\partial P_i}{\partial t} &= \underbrace{(1-\delta^{P_i})\mu^{P_i}P_i}_{production} - \underbrace{m^{P_i}\frac{P_i}{K_P+P_i}P_i}_{mortality} \\ &- \underbrace{w_{agg}^{P_i}P_i^2}_{aggregation\ loss} - \underbrace{\sum_j g_{P_i}^{Z_j}Z_jP_i}_{grazing\ loss}\end{aligned} \tag{2}$$

where δ^{P_i} is the fraction of primary production (PP) converted into DOC, m^{P_i} is the mortality rate of P_i, K_p is the half-saturation constant for mortality and ω_{agg}^P is the density dependent loss rate. $g_{P_i}^{Z_j} * Z_j * P_i$ describes the amount of biomass lost in grazing by the zPFT $Z_j, j \in \{1,3\}$. μ_P is the phytoplankton growth rate and is a function of temperature, light and nutrient availability. In the model, the growth rate is calculated as:

$$\begin{aligned}\mu^{P_i} &= \mu_0^{P_i} * f(T) * f(PAR) * f(nut) \\ &= \mu_0^{P_i} * b^T * (1-e^{-\alpha^{P_i}PAR}) * (1-\gamma(lpf))\, L_{lim}^{P_i}\end{aligned} \tag{3}$$

where $\mu_0^{P_i}$ is the maximum growth rate at 0° C,a b is the temperature dependence of the growth rate and T is the temperature. α^{P_i} is the coefficient of the initial slope of the dependence of photosynthesis on light intensity and varies for each pPFT. This coefficient is parametrised as

$$\alpha^{P_i} = \frac{1 + ldp * e^{-0.21PAR}}{20} \tag{4}$$

where PAR is the Photosynthetic Available Radiation and ldp is the light dependency of photosynthesis. PAR is the sum of green, PAR_g, and red, PAR_r light:

$$\begin{aligned}PAR(z) &= PAR_g(z) * e^{(-x_g + .074\sum_{j=1}^{6} CHL^{.674})} \\ &+ PAR_r(z) * e^{(-x_r + .037\sum_{j=1}^{6} CHL^{.629})}\end{aligned} \tag{5}$$

$\gamma(lpf)$ is a PFT-dependent factor affecting phytoplankton growth depending on the light penalty function (lpf), i.e., calculation of the phytoplankton growth rate takes into account that light availability is affected by vertical mixing. If the mixed layer depth is shallower than the euphotic zone, then $\gamma(lpf) = 0$, which means that the growing algae get no penalty. If the mixed layer depth is more than twice the euphotic zone, then $\gamma(lpf)$ is at its parameterised maximum and simulates a proportionality coefficient between algal growth and the time algae spend in the dark (André, 1990). If the mixed layer depth is between one and two times the euphotic zone depth, the penalty is linearly interpolated between these two cases.
The nutrient limitation ($L_{lim}^{P_i}$) determines the limitation of the growth rate due to the availability of nutrients. It is assumed that nutrient limitation follows Michaelis-Menten kinetics and that growth is determined by the least available nutrient. Hence, for P = phytoplankton other than the silicifiers

$$L_{lim}^{P_i} = \min\left(\frac{PO_4}{K_{PO_4}^{P_i}+PO_4}, \frac{Fe}{K_{Fe}^{P_i}+Fe}\right) \tag{6}$$

and for silicifiers (D= diatoms)

$$L_{lim}^{D} = \min\left(\frac{PO_4}{K_{PO_4}^{D}+PO_4}, \frac{Fe}{K_{Fe}^{D}+Fe}, \frac{Si}{K_{Si}^{D}+Si}\right), \tag{7}$$

In PlankTOM10 dissolved inorganic nitrogen is included so these relationships become, except for nitrogen fixers:

$$L_{lim}^{P_i} = \min\left(\frac{PO_4}{K_{PO_4}^{P_i}+PO_4}, \frac{Fe}{K_{Fe}^{P_i}+Fe}, \frac{DIN}{K_{DIN}^{P_i}+DIN}\right) \tag{8}$$

and for silicifiers

$$L_{lim}^{DIA} = \min\left(\frac{PO_4}{K_{PO_4}^{DIA}+PO_4}, \frac{Fe}{K_{Fe}^{DIA}+Fe}, \frac{DIN}{K_{DIN}^{DIA}+DIN}, \frac{Si}{K_{Si}^{DIA}+Si}\right), \tag{9}$$

Phytoplankton mortality rates are proportional to the availability of the limiting nutrient and are described as:

$$m^{P_i} \quad = \quad m_{min}^{P_i} + (m_{max}^{P_i} - m_{min}^{P_i}) * \min\left(1, \frac{PO4}{K_{PO4}^{P_i}}, \frac{FER}{K_{Fe}^{P_i}}, \frac{SIL}{K_{SIL}^{P_i}}, \frac{DIN}{K_{DIN}^{D}}\right). \tag{10}$$

The density specific loss rate is constant for all PFT except silicifiers. For these, aggregation is enhanced under nutrient limiting conditions as follows:

$$w_{agg}^{D} \quad = \quad w_{min} + w_{max} * \left(1 - \min\left(\frac{PO_4}{K_{PO_4}^{D}}, \frac{Fe}{K_{Fe}^{D}}, \frac{Si}{K_{Si}^{D}}, \frac{DIN}{K_{DIN}^{D}}\right)\right). \tag{11}$$

The term describing the loss of phytoplankton biomass due to zooplankton grazing will be explained in Section 4.

Table 3: List of Parameters used in evolution of phytoplankton

Term	**Variable**	**Description**	**Where set**
δ^{P_i}	rn_docphy	fraction of primary production converted to DOC	*sms.F90*
$\mu^{P_i} P_i$	prophy	productivity of phytoplankton P_i	*bgcnul,bgcpro*
$\mu^{P_{i_0}}$	rn_mumpft	maximum growth rate at 0^oC	*namelist.trc.sms*
b^T	rn_mutpft	temperature dependence of growth rate	*namelist.trc.sms*
α^{P_i}	pislope^{-1}	initial slope of PI curve	*bgcpro*
PAR	etot	Photosynthetcally active radiation	*bgcpro*
ldp	rn_mulphy	light dependence of photosynthesis	*namelist.trc.sms*
$\gamma(lpf)$	rn_mupphy	penalty for P_i growth where mixed layer depth $>$ euphotic depth, else =1	*namelist.trc.sms*
x_g	rn_ekwgrn	absorption coefficient of water for green light	*namelist.trc.sms*
x_r	rn_ekwred	absorption coefficient of water for red light	*namelist.trc.sms*
$K_{FER}^{P_i}$	rn_kmfphy	half-saturation coefficients for FER	*namelist.trc.sms*
$K_{DIN}^{P_i}$	rn_kmnphy	half-saturation coefficients for DIN	*namelist.trc.sms*
$K_{PO4}^{P_i}$	rn_kmpphy	half-saturation coefficients for $PO4$	*namelist.trc.sms*
K_{SIL}^{DIA}	rn_sildia	half-saturation coefficients for SIL in diatoms	*namelist.trc.sms*
$m_{min}^{P_i}$	rn_momphy	minimum mortality of P_i	*namelist.trc.sms*
$m_{max}^{P_i}$	rn_morphy	maximum mortality of P_i	*namelist.trc.sms*
m^{P_i}	dyphy	mortality rate of P_i	*bgclos*
w_{agg}	rn_resphy	density dependent loss rate	*namelist.trc.sms*
w_{agg}^{D}	wchlp	density dependent loss rate for diatoms	*bgclos*
w_{min}	rn_resphy	min. density dependent loss rate for diatoms	*namelist.trc.sms*
w_{max}	0.1	max. density dependent loss rate for diatoms	*bgclos*

3.2 Primary Production, Photosynthesis and Chlorophyll - DCH, NCH, CCH, PCH, HCH, FCH

The photosynthesis model is in the process of being changed.

3.2.1 The old formulation (as in PISCES)

The chlorophyll content of each phytoplankton type (DCH for silicifiers, NCH for mixed-phytoplankton, CCH for calcifiers and PCH for picophytoplankton, HCH for DMSp and FCH for N_2-fixers) is modelled. Chlorophyll evolves in a very similar fashion to phytoplanktonic biomass (see equation 2), as sources and sinks of chlorophyll are of phytoplanktonic origin. It is calculated with the steady state solution to the photosynthesis model of Geider et al. (1996):

$$\begin{aligned}\frac{\partial Chl^{P_i}}{\partial t} &= \underbrace{\rho_{Chl}^{P_i}(1-\delta^{P_i})\mu^{P_i}P_i}_{production\ by\ phytoplankton} - \underbrace{m^{P_i}\frac{P_i}{K_{P_i}+P_i}Chl^{P_i}}_{phytoplankton\ mortality} \\ &- \underbrace{w_{agg}^{P_i}P_i Chl^{P_i}}_{aggregation} - \underbrace{\Sigma g_j^{zoo}(P_i)\theta_{Chl}^{P_i}Z_j}_{grazing},\end{aligned} \tag{12}$$

where Chl^{P_i} is the chlorophyll-a concentration and $\theta_{chl}^{P_i}$ the chlorophyll to carbon ratio of P_i. $\rho_{chl}^{P_i}$ represents the energy efficiency of P_i (ratio of energy assimilated by P_i to energy absorbed) after the model of Geider et al. (1996). In the model, the latter two functions are calculated as

$$\rho_{chl}^{P_i} = \theta_{chl,max}^{P_i}\frac{144\mu^{P_i}}{\alpha_{chl}^{P_i} * PAR * \theta_{chl}^{P_i}} \tag{13}$$

$$\theta_{chl}^{P_i} = \left(\frac{Chl^{P_i}}{P_i}\right). \tag{14}$$

where 144 is the square of the molar mass of carbon and is used to convert from mol to g. $\alpha_{chl}^{P_i}$ is modified from the α^{P_i} used in the evolution of biomass as:

$$\alpha_{Chl}^{P_i} = 0.6 * b^T * 55 * \alpha^{P_i} \tag{15}$$

$$\tag{16}$$

The mortality aggregation and grazing terms leave the phytoplankton Chl:C ratio unchanged.

3.3 The new model (adapted from (Geider et al., 1998))

The iron-light colimitation model is a dynamical photosynthesis model in which the rate of photosynthesis both controls cellular iron and chlorophyll synthesis and is controlled by their quota (Buitenhuis and Geider in prep.).

Chapter 4

Heterotrophic PFT's

The temporal evolution of zooplankton and the pico-heterotrophs are shown in Figure 4.

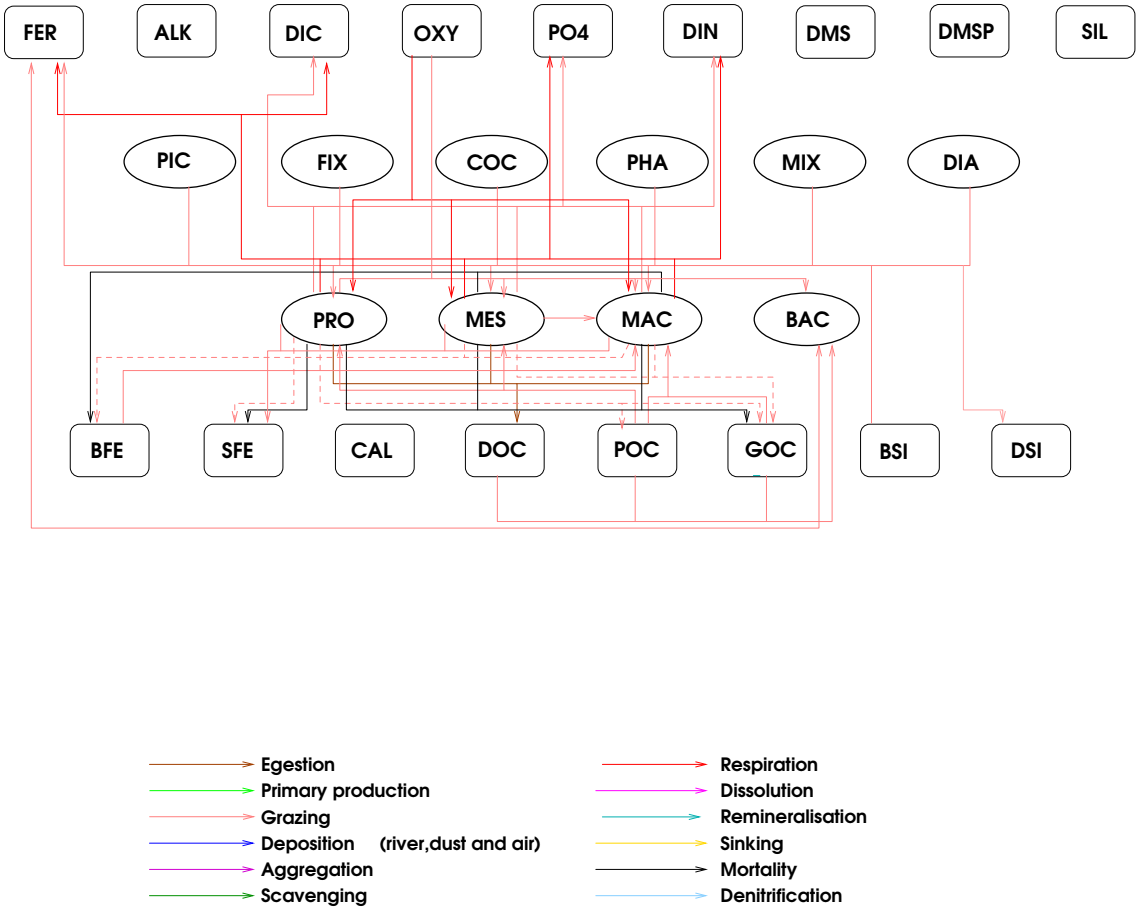

Figure 4: The processes governing the development of the zooplankton and pico-heterortrophs.

4.1 Zooplankton Biomass - PRO, MES and MAC

The temporal evolution of zooplankton concentrations Z_j in PlankTOM are described as follows (Buitenhuis et al., 2006a):

$$\frac{\partial Z_j}{\partial t} = \underbrace{\sum_k g_{F_k}^{Z_j} * F_k * MGE * Z_j}_{growth\ through\ grazing} - \underbrace{\sum_{k=j+1}^{3} g_{Z_j}^{Z_k} * Z_k}_{loss\ through\ grazing} - \underbrace{R_{0^\circ}^{Z} * d^T * Z_j}_{basal\ respiration} - \underbrace{m_{0^\circ}^{Z_j} * c_{Z_j}^{T} * Z_j}_{mortality}, \quad (17)$$

where $R_{0^\circ}^{Z}$ is the respiration rate at 0°C, d is the temperature dependence of the respiration ($d^{10} = Q_{10}$).,$m_{0^\circ}^{Z}$ is the mortality rate at 0°C, c_{Z_j} is the temperature dependence of the mortality ($c^{10} = Q_{10}$), and $\beta \in 1, 2$ is the exponent for biomass, with $\beta = 1$ in PlankTOM10.
The growth term is described in detail below.

4.1.1 Grazing rate

Grazing $g_{F_k}^{Z_j}$, of zooplankton Z_j on food source F_k is dependent on the zooplankton preference, $p_{F_k}^{Z_j}$, the concentration of the food source and the temperature. H^{Z_j} is the threshold concentration below which zooplankton starve and $K_{1/2}^{Z}$ is the half-saturation constant for grazing,

$$g_{F_k}^{Z_j} = g_{max}^{Z_j}(T) \frac{p_{F_k}^{Z_j} \left(1 - \frac{H^{Z_j}}{\sum_k p_{F_k}^{Z_j} F_k}\right)}{K^{Z_j} + \sum_i p_{F_k}^{Z_j} F_k - H^{Z_j}} \quad (18)$$

The food sources F for zooplankton are summarised in Table 4. For macro-zooplankton they are phytoplankton, meso-zooplankton, proto-zooplankton, small and large particulate organic matter (for the effect of variable Fe:C ratios, see equation 53). The food sources F for meso-zooplankton are phytoplankton, proto-zooplankton and small particulate organic matter. The food sources for proto-zooplankton are phytoplankton, bacteria and small particulate organic matter.

Table 4: Food sources for zooplankton and pico-heterotrophs

Food	Macro-zooplankton	Meso-zooplankton	Proto-zooplankton	Pico-heterotrophs
Meso-zooplankton	*			
Proto-zooplankton	*	*		
Phytoplankton	*	*	*	
Pico-heterotrophs			*	
Large POM	*			*
Small POM	*	*	*	*
Dissolved OM				*

The temperature dependence of the grazing rate is:

$$g_{max}^{Z_j}(T) = g_{0^\circ}^{Z} b^T, \quad (19)$$

where $g_{0^\circ}^{Z}$ is the maximum grazing rate at 0° C, b is the temperature dependence of the grazing rate ($b^{10} = Q_{10}$), T is the local seawater temperature in °Celsius.

The model growth efficiency MGE is a a function of gross growth efficiency (GGE), which describes the fraction of grazed food incorporated into zooplankton biomass and basal respiration normalised to all material ingested:

$$MGE = GGE + \frac{R_{0^\circ}^{Z} * d^T * Z_j}{\sum_{F_i} g_F^Z}. \quad (20)$$

Table 5: List of Parameters used in evolution of zooplankton

Term	Variable	Description	Where set
g_0^Z	rn_gramic	maximum grazing rate at 0^o	*namelist.trc.sms*
	rn_grames	for micro, meso-zooplankton	*namelist.trc.sms*
	rn_gramac	and macro-zooplankton	*namelist.trc.sms*
b	rn_mutpft	Temperature dependence of growth	*namelist.trc.sms*
		for micro, meso-zooplankton	*namelist.trc.sms*
		macro-zooplankton	*namelist.trc.sms*
p_F^Z	rn_gmibac	proto-zoo. grazing preference for bacteria	*namelist.trc.sms*
	rn_gmigoc	proto-zoo. grazing preference for GOC	*namelist.trc.sms*
	rn_gmipoc	proto-zoo. grazing preference for POC	*namelist.trc.sms*
	rn_gmiphy	proto-zoo. grazing preference for phyto.	*namelist.trc.sms*
	rn_gmegoc	meso-zoo. grazing preference for GOC	*namelist.trc.sms*
	rn_gmepoc	meso-zoo. grazing preference for POC	*namelist.trc.sms*
	rn_gmemic	meso-zoo. grazing preference for proto-zoo.	*namelist.trc.sms*
	rn_gmephy	meso-zoo. grazing preferencefor phyto	*namelist.trc.sms*
	rn_gmabac	macro-zoo preference for bacteria	*namelist.trc.sms*
	rn_gmagoc	macro-zoo preference for GOC	*namelist.trc.sms*
	rn_gmames	macro-zoo preference for meso-zoo	*namelist.trc.sms*
	rn_gmamic	macro-zoo preference for proto-zoo	*namelist.trc.sms*
	rn_gmapoc	macro-zoo preference for POC	*namelist.trc.sms*
	rn_gmaphy	macro-zoo preference for each phyto. type	*namelist.trc.sms*
K^{Z_j}	rn_grkmic	half-saturation constant for	*namelist.trc.sms*
	rn_grkmes	micro, meso-zooplankton	*namelist.trc.sms*
	rn_grkmac	and macro-zooplankton	*namelist.trc.sms*
H^{Z_j}	rn_grmmic	grazing threshold for proto-	*namelist.trc.sms*
	rn_grmmes	meso- and	*namelist.trc.sms*
	rn_grmmac	macro-zooplankton	*namelist.trc.sms*
$R_{0^\circ}^Z$	rn_resbac	respiration at 0°C	*namelist.trc.sms*
	rn_resmic	of bacteria, proto-zooplankton,	*namelist.trc.sms*
	rn_resmes	meso-zooplankton	*namelist.trc.sms*
	rn_resmac	and macro-zooplankton	*namelist.trc.sms*
d^T	rn_retbac	Temperature dependence of respiration	*namelist.trc.sms*
	rn_retmic	of bacteria, proto-zooplankton,	*namelist.trc.sms*
	rn_retmes	meso-zooplankton	*namelist.trc.sms*
	rn_retmac	and macro-zooplankton	*namelist.trc.sms*
$m_{0^\circ}^Z$	rn_mormes	mortality at 0°C of meso-zoo.	*namelist.trc.sms*
	rn_mormac	and macro-zooplankton	*namelist.trc.sms*
$c_{Z_j}^T$	rn_motmes	temperature dependence of mortality	*namelist.trc.sms*
	rn_motmac	for meso and macro-zooplankton	*namelist.trc.sms*
GGE^Z	rn_ggemic	Growth efficiency	*namelist.trc.sms*
	rn_ggemes	of micro,meso and	*namelist.trc.sms*
	rn_ggemac	macro-zooplankton	*namelist.trc.sms*
MGE^Z	micrge	Model growth efficiency	*bgcbio,bgclos*
	mesoge	of micro,meso and	*bgcbio,bgclos*
	macrge	macro-zooplankton	*bgcbio,bgclos*

4.2 Pico-heterotrophs

The temporal evolution of bacterial concentration is modelled in a similar way to zooplankton:

$$\frac{\partial BAC}{\partial t} = \underbrace{M^{bac}_{max}(T) * \frac{\eta_O * \sum_k p^{BAC}_{F_k} F_k}{K_{org} + \sum_k p^{BAC}_{F_k} F_k} * BGE * BAC}_{mineralisation} \tag{21}$$

$$- \underbrace{R_{0^\circ} * d^T * BAC}_{respiration} - \underbrace{\sum_j g^{Z_j}_{BAC} * BAC * Z_j}_{grazing} \tag{22}$$

where BAC is the bacterial concentration and BGE is the bacterial growth efficiency. The food sources F_k for bacteria are DOC and small and large particulate organic carbon. Each food source is associated with a preference p^{BAC}_F. Mineralisation rate $M_{max}(T)$ is temperature dependent:

$$M_{max}(T) = M_{0^\circ} * b^T, \tag{23}$$

where M_{0° is the maximum mineralisation rate at 0° C, b is the temperature dependence of the mineralisation rate ($b^{10} = Q_{10}$) and T is the local seawater temperature in °Celsius.K_{org} is the half-saturation constant for mineralisation. Bacterial growth is dependent on the available oxygen: $\eta_O = \frac{OXY+3*10^{-6}}{OXY+10*10^{-6}}$, which leads to a maximum bacterial growth rate in the absence of oxygen that is 0.3 times the maximum growth rate at high oxygen.

R_{0° is the respiration rate at 0°C, d is the temperature dependence of the respiration ($d^{10} = Q_{10}$).

Bacterial growth efficiency BGE, which describes the fraction of mineralised food incorporated into bacterial biomass, is a function temperature and iron availability :

$$BGE = \frac{min(BGE_{0^\circ} - e * T, FER_{BAC} + \lambda^*_{POC} Fe + \lambda^*_{GOC} Fe)}{max((\lambda^*_{DOC} DOC + \lambda^*_{POC} POC + \lambda^*_{GOC} GOC) * Fe/C, 1e-25)} \tag{24}$$

where BGE_{0° is the bacterial growth efficiency at 0° and e is the temperature dependence of bacteria growth, Fe_{BAC} is the uptake of dissolved Fe and $\lambda^*_{GOC}, \lambda^*_{DOC}, \lambda^*_{POC}$ are the remineralisation rates for DOC, GOC and POC respectively.

4.2.1 Bacterial degradation in PlankTOM5

PlankTOM5 does not include an explicit formulation for bacterial biomass. We use an implicit formulation following Aumont and Bopp (2006b), where bacterial biomass is a function of zooplankton biomass, folded by a depth profile (see below). Bacterial degradation is parametrised using simulated biomass and a bacterial activity on sulphur compound S_{com}. Thus,

$$\phi^{bac}_{S_{com}} = \mu^{bac} * L^{bac}_{tot} * f(T) * BAC, \tag{25}$$

with μ^{bac} is the maximal bacterial growth rate, L^{bac}_{tot} the total nutrient limitation for bacteria, $f(T)$ the temperature dependence of growth and BAC the simulated bacterial biomass. The bacterial temperature dependence has been chosen as a $Q_{10} = 3$. The individual terms are calculated as

$$L^{bac}_{tot} = \min\left(L^{bac}_{nut}, \frac{S_{com}}{S_{com} + K^{S_{com}}}\right) * bac^{light}_{limi} \tag{26}$$

$$L^{bac}_{nut} = \min\left(\frac{PO_4}{PO_4 + K^{PO_4}}, \frac{Fe}{Fe + K^{Fe}}, \frac{DOC}{DOC + K^{DOC}}\right) \tag{27}$$

$$bac^{light}_{limi} = \min\left(1., \max\left(0.66, 1. - (\frac{PAR}{PAR_{max}})^6 + 0.18\right)\right) \tag{28}$$

$$f(T) = 1.116^T \tag{29}$$

$$BAC = \frac{0.7 * (MIC + 2 * MES)}{B_{norm}} * \min\left(1, \frac{depth(12)}{depth}\right), \tag{30}$$

with L^{bac}_{nut} the bacterial nutrient limitation of the model, excluding S_{com}, bac^{light}_{limi} the bacterial limitation of S_{com} degradation as a function of insolation (Slezak et al., 2001) and all biomasses as defined above. Bacterial activity is a function of the nutrient availability of both DOM and S_{com} and parametrised using the minimum of 4 independent Michaelis-Menten functions, with PO_4 phosphate, Fe iron and DOC dissolved organic matter concentrations. The K^{nut} are the half-saturation constants for bacteria on the respective nutrient S_{com}.

Grazing of bacteria by zooplankton is described earlier in the previous section..

Table 6: List of Parameters used in evolution of pico-heterotrophs

Term	Variable	Description	Where set
K_{org}	rn_kmobac	Half saturation constant for mineralisation	*namelist.trc.sms*
BGE_{0°	rn_ggebac	Bacterial growth efficiency at 0°	*namelist.trc.sms*
e	rn_ggtbac	Temperature dependence of bacterial growth	*namelist.trc.sms*
FER_{BAC}	ubafer	Uptake of dissolved Fe by bacteria	*bgcsnk*
η_O	$\frac{OXY+3*10^{-6}}{OXY+10*10^{-6}}$	oxygen limitation to bacteria growth	
$\lambda^*_{POC}Fe$	ofer	remineralisation of Fe in POC	*bgcsnk*
$\lambda^*_{GOC}Fe$	ofer2	remineralisation of Fe in GOC	*bgcsnk*
$\lambda^\star_{DOC}DOC$	olimi	remineralisation of DOC	*bgcnul ,bgcsnk*
$\lambda^\star_{POC}POC$	orem	remineralisation of POC	*bgcnul ,bgcsnk*
$\lambda^\star_{GOC}GOC$	orem2	remineralisation of GOC	*bgcnul ,bgcsnk*

4.2.2 Denitrification

When waters become suboxic, bacteria can also use nitrate in order to gain oxidative power for DOC remineralization. Hence, there is a (bacterial) denitrification term in the model.

Chapter 5

Organic matter and bacterial remineralisation

The source and sinks for dissolved organic carbon (DOC) and small (POC) and large (GOC) particulate carbon are shown in Figure 5

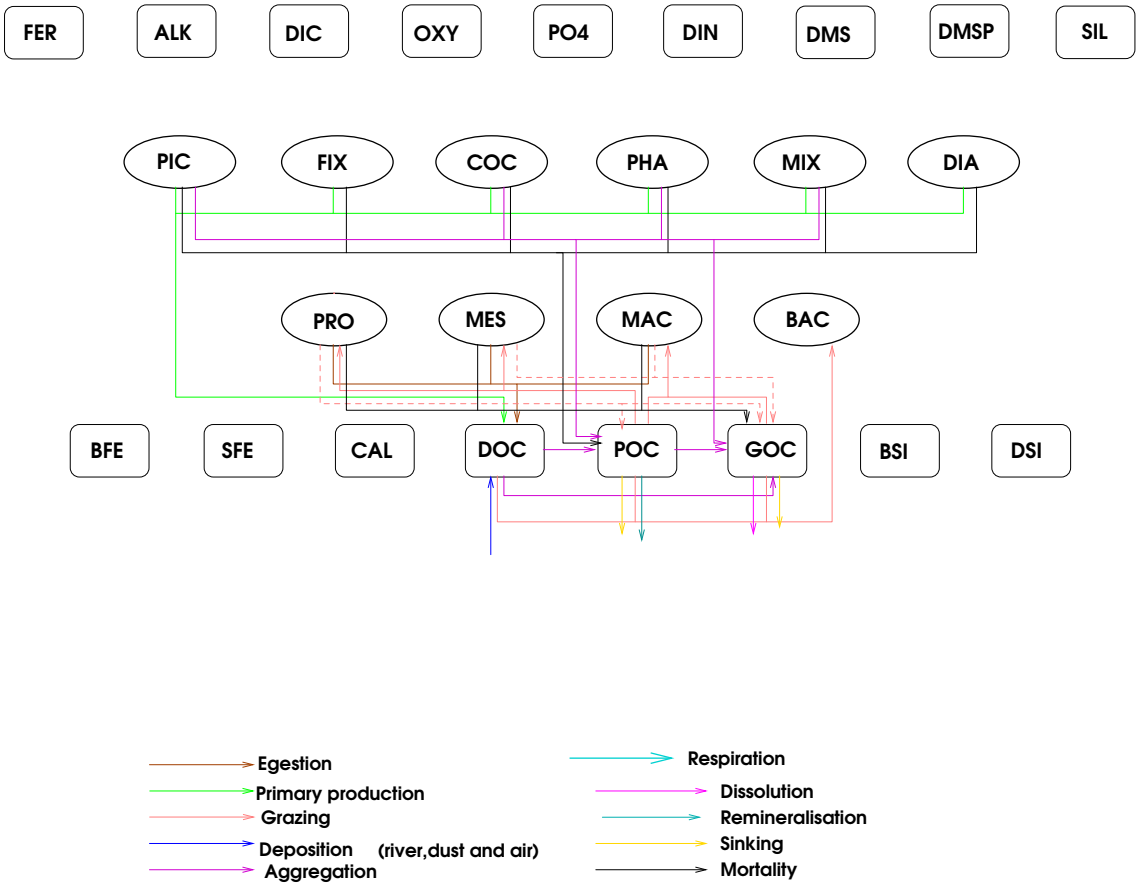

Figure 5: The source and sinks for dissolved organic carbon (DOC) and small (POC) and large (GOC) particulate carbon.

5.1 Dissolved organic carbon - DOC

PlankTOM5 Note
Bacterial remineralization is implicitly modelled as a function of temperature and of the concentration of dissolved organic matter. An implicit bacterial remineralisation converts DOC to inorganic nutrient and cleaves small and large POM to DOC and Fe. The organic substrates for bacterial remineralization are dissolved organic carbon (DOC) and small and large particulate organic carbon (POC and GOC).
The temporal evolution of DOC concentration is modelled as follows:

$$\begin{aligned}\frac{\partial DOC}{\partial t} &= \underbrace{\sum \delta^{P_i}\mu^{P_i}P_i}_{production} + \underbrace{\sum_j \left[(1-\sigma^{Z_j})(1-\xi^{Z_j}-MGE^{Z_j})\sum_k g^{Z}_{F_k} * Z_j * F_k\right]}_{zooplankton\ dissolved\ egestion} \\ &+ \underbrace{\lambda^{\star}_{POC}POC}_{bacterial\ POC\ conversion} - \underbrace{\lambda^{\star}_{DOC}DOC}_{bacterial\ degradation} \\ &- \underbrace{\Phi^{DOC\rightarrow POC}_{agg} - \Phi^{DOC\rightarrow GOC}_{agg}}_{aggregation} + \underbrace{DOC_{riv}}_{river\ input\ of\ DOC}\ ,\end{aligned} \tag{31}$$

where δ^{P_i} is the fraction of primary production converted to DOC , μ^{P_i} is the phytoplankton growth rate , (1-σ^{Z}) is the fraction of zooplankton ingested food converted to DOC , ξ^{Z_j} is the fraction of unassimilated food , MGE_j is the model growth efficiency of zooplankton , $g^{Z_j}_{F_i}$ is as in equation (17).
$\lambda^{\star}_{POC}$ and $\lambda^{\star}_{DOC}$ are the bacterial degradation rates of DOC and POC, respectively.

$$\begin{aligned}\lambda^{\star}_{DOC} &= \lambda_{DOC} * L^{bac}_{lim} P^{z=0}_{tot} \max\left(0.1, e^{\frac{max(0,z-50)}{100}}\right) \\ \lambda^{\star}_{POC} &= \lambda_{POC}\eta_O \\ L^{bac}_{lim} &= \min\left(\frac{DOC}{K^{bac}_{DOC}+DOC}, \frac{PO4}{K^{bac}_{PO4}+PO4}, \frac{Fe}{K^{bac}_{Fe}+Fe}\right)\end{aligned} \tag{32}$$

where $P^{z=0}_{tot}$ is the surface phytoplankton concentration, and z is depth.

In PlankTOM10 the bacterial biomass is modelled and $\frac{\partial DOC}{\partial t}$ is calculated in *bgcbio* in the following way:

$$\begin{aligned}\frac{\partial DOC}{\partial t} &= \underbrace{\sum \delta^{P_i}\mu^{P_i}P_i}_{production} + \underbrace{\sum_j \left[(1-\sigma^{Z_j})(1-\xi^{Z_j}-MGE^{Z_j})\sum_k g^{Z_j}_{F_k} * Z_j * F_k\right]}_{egestion} \\ &- \underbrace{\lambda^{\star}_{DOC}DOC}_{bacterial\ degradation} \underbrace{- \Phi^{DOC\rightarrow POC}_{agg} - \Phi^{DOC\rightarrow GOC}_{agg}}_{aggregation} \\ &+ \underbrace{DOC_{riv}}_{river\ input}\ ,\end{aligned} \tag{33}$$

Bacterial degradation is calculated in *bgcnul* and *bgcsnk* according to the equations:

$$\lambda^{\star}_{DOC}DOC = p^{bac}_{DOC} * DOC * \lambda^{\star}_{OC}OC \tag{34}$$

and

$$\lambda^{\star}_{OC}OC = \frac{\mu^{bac}_{0^\circ}b^T * \eta_O * BAC}{(K^{bac}_{DOC} + \sum_k p^{bac}_{F_k}F_k)} \tag{35}$$

where F_k is DOC, POC and GOC. η_O = $\frac{3*10^{-6}+OXY}{OXY+10^{-6}}$ leads to a maximum bacterial growth rate in the absence of oxygen that is 0.3 times the maximum growth rate at high oxygen.

The aggregation functions $\Phi^{X\rightarrow Y}_{agg}$ are described in Section 5.2.

Table 7: List of Parameters used in bacterial remineralisation of DOC

Term	Variable	Description	Where set
σ^{Z_j}	rn_sigmic	Fraction of zooplankton	*namelist.trc.sms*
	rn_sigmes	excretion as DIC	
	rn_sigmac		
$(1-\xi^{Z_j}-GGE^{Z_j})*$	grarem	remineralisation due	*bgclos*
$\sum_{F_i} g_{F_i}^{Z_j} Z_j$	grarem2	to grazing by micro, meso	
	grarem3	and macro-zooplankton	
ξ^{Z_j}	rn_unamic	Fraction of unassimilated	*namelist.trc.sms*
	rn_unames	food by micro, meso	
	rn_unamac	and macro-zooplankton	
MGE^{Z_j}	micrge	model growth of efficiency	
	mesrge	of micro, meso and	
	macrge	macro-zooplankton	
$g_{F_i}^{Z_j} Z_j$	gramit	Total grazing by	*bgclos*
	gramet	micro,meso and	
	gramat	macro-zooplankton	
$\lambda^{\star}_{POC} POC$	orem *rn_sigpoc	Remineralisation rate of POC	
		to DOC (PlankTOM5 only)	*bgcnul ,bgcsnk*
L_{lim}^{bac}	xlimbac	Nutrient limit to bacteria	*bgcsnk,bgcpro*
$P_{tot}^{z=0}$	phymoy	phyto. surface concentration	*bgcsnk bgcpro*
K_{DOC}^{BAC}	rn_kmobac	DOC half saturation constant	*namelist.trc.sms*
K_{PO4}^{BAC}	rn_kmpbac	PlankTOM: PO4 half saturation constant	*namelist.trc.sms*
K_{FER}^{BAC}	rn_kmfbac	FER half saturation constant	*namelist.trc.sms*
$\mu_{0^\circ}^{bac}$	rn_mumpft	growth rate of bacteria at 0°	*namelist.trc.sms*
b	rn_mutpft	temp. dependence of growth rate	*namelist.trc.sms*
p_F^{bac}	rn_gbadoc	bacterial preference for DOC	*namelist.trc.sms*
	rn_gbapoc	POC	*namelist.trc.sms*
	rn_gbagoc	GOC	*namelist.trc.sms*
λ_{DOC}	$1.64 * .003$+rn_degdoc	PlankTOM5: DOC remineralisation rate	*namelist.trc.sms*
λ_{POC}	rn_degpom *rn_sigpoc	PlankTOM5	*namelist.trc.sms*
DOC_{riv}	depdoc	River input of DOC	*trcini.dgom*

5.2 Particulate aggregation

Particle aggregation through either differential sinking or turbulent coagulation is calculated by:

$$\begin{aligned}
\Phi_{agg}^{DOC\rightarrow POC} &= \phi_1^{DOC}\epsilon DOC^2 + \phi_2^{DOC}\epsilon DOC\, POC \\
\Phi_{agg}^{DOC\rightarrow GOC} &= \phi_3^{DOC}\epsilon\, DOC\, GOC \\
\Phi_{agg}^{POC\rightarrow GOC} &= \phi_1^{POC}\epsilon POC^2 + \phi_2^{POC}\epsilon GOC\, POC \\
&\quad +\phi_3^{POC} POC\, GOC + \phi_4^{POC} POC^2
\end{aligned} \tag{36}$$

In which ϵ is the shear rate. It is set to 1.0 s^{-1} in the mixed layer and to 0.01 s^{-1} elsewhere. The coefficients ϕ were obtained by integrating the standard curvilinear kernels for collisions over the size range of each organic matter pool.

Table 8: List of Parameters used in particulate aggregation

Term	Variable	Description	Where set
$\Phi_{agg}^{DOC\rightarrow POC}$	xaggdoc	DOC-POC aggregation	*bgcsnk*
$\Phi_{agg}^{DOC\rightarrow GOC}$	xagg2doc	DOC-GOC aggregation	*bgcsnk*
ϕ_1^{DOC}	rn_ag5doc		*namelist.trc.sms*
ϕ_2^{DOC}	1000.		
ϕ_3^{DOC}	rn_ag6doc		*namelist.trc.sms*
ϕ_1^{POC}	rn_ag1poc		*namelist.trc.sms*
ϕ_2^{POC}	rn_ag2poc		*namelist.trc.sms*
ϕ_3^{POC}	rn_ag3poc		*namelist.trc.sms*
ϕ_4^{POC}	rn_ag4poc		*namelist.trc.sms*

5.3 Sinking

The sinking speed V_{sink} [m/d] of GOC, $CaCO_3$ and SiO_2 [mol/L] is calculated using the drag equation as in Buitenhuis et al. (2001):

$$V_{sink} = \left(\frac{2 * V * g * (\rho_{particle} - \rho_{seawater})}{A * \rho_{seawater} * C_d}\right)^{0.5} \tag{37}$$

$$Re = \frac{V_{sink} * \rho_{seawater} * r}{\eta} \tag{38}$$

$$C_d = I * Re^{\pi} \tag{39}$$

In which V is the volume of the particle, g the gravitational constant, ρ the density, A the surface area of the particle, C_d the drag coefficient, Re the Reynolds number, r the radius of the particle, η the kinematic viscosity, and I and π are empirical parameters which were taken from Alldredge and Gotschalk (1988). The density of the particle is calculated as in Buitenhuis et al. (2001), assuming that the contribution of SiO_2 to the porosity of the particle is the same as for $CaCO_3$. The specific weight of $CaCO_3$ was taken as 2800000 g m^-3 and of SiO_2 as 2100000 g m^{-3} :

$$\rho_{particle} = \frac{(GOC * 24. + CaCO_3 * 100. + SiO_2 * 60.) * 10^3}{\max(\frac{GOC*24.}{1040.380} + \frac{CaCO_3*100.}{1660.000} + \frac{SiO_2*60.}{1245.000}, 10^{-15})} \tag{40}$$

These equations were solved offline by iteration. The radius r of the particles (162 μ m) and the density of organic matter (ρ_{min} = 1040380 g m^{-3}) were chosen in such a way that the sinking speed of organic matter is 3 m d^{-1} (the sinking speed of POC, S_{poc}) and that the average concentrations of GOC, $CaCO_3$ and SiO_2 at 100m. depth (from the PlankTOM 5 model without ballasting, Le Quéré et al. 2005) resulted in a sinking speed of 50 m d^{-1}.

This offline calculation gives the relationship between the density of particles $\rho_{particle}$ and sinking speed.

$$V_{sink} \quad = \quad S_{poc} + S_{goc} * (e^{\frac{MIN(\rho_{particle},\rho_{max})-\rho_{min}}{k_{goc}}} - 1), \tag{41}$$

where ρ_{max} is the density at which the sinking speed is 150 m d^{-1} (the maximum that is numerically stable with 15 timesteps per day and water layers that are 10 m. deep at the surface). This could be well fitted (for $\rho_{particle} < 1091314 : R^2 = 0.999$) by S_{poc} = 3, S_{goc} =20 and k_{goc} = 24000.

Table 9: List of Parameters used in sinking

Term	Variable	Description	Where set
S_{poc}	rn_snkpoc	sinking speed of POC	*namelist.trc.sms*
S_{goc}	rn_snkgoc	sinking speed parameter for GOC	*namelist.trc.sms*
k_{goc}	rn_singoc	second sinking speed parameter for GOC	*namelist.trc.sms*
ρ_{min}	dnsin	density at which sinking speed is 3m d^{-1}	*trclsm.dgom.h90*
ρ_{max}	dnsmax	density at which sinking speed is 150m d^{-1}	*trclsm.dgom.h90*
$\rho_{particle}$	xdens	density of particle	*bgcsnk*

5.4 Small particulate organic carbon - POC

The temporal evolution of small POC (POC) is calculated as as

$$\begin{aligned}\frac{\partial POC}{\partial t} \quad = \quad & \underbrace{\xi^{mic} * (\sum_{F_i} g_{F_i}^{mic} Z_{mic})}_{proto-zooplankton\ unassimilated\ food} - \underbrace{\sum_{Z_j} g_{POC}^{Z_j} * Z_j * POC}_{grazing\ on\ POC} + \underbrace{\sum_{P_i} m^{P_i} \frac{P_i}{K_{P_i} + P_i} P_i}_{phytoplankton\ mortality} \\ & + \underbrace{\sum_{PHA,PIC,MIX,COC} w_{agg}^{P_i} P_i^2}_{aggregation\ to\ POC} - \underbrace{\lambda_{POC}^{\star} POC}_{POC\ remineralisation} - \underbrace{S_{POC} \frac{\partial POC}{\partial z}}_{POC\ sinking} \\ & + \underbrace{\Phi_{agg}^{DOC \to POC}}_{aggregation\ to\ POC} - \underbrace{\Phi_{agg}^{POC \to GOC}}_{aggregation\ to\ GOC} + \underbrace{POC_{riv}}_{river\ input} .\end{aligned} \tag{42}$$

Here, ξ^{mic} is the unassimilated fraction of grazed material, $g_{F_i}^{mic}$ are the grazing coefficients of proto-zooplankton on food sources F as specified in (17), m^{P_i} is plankton mortality as in (2 and 10), $w_{agg}^{P_i}$ is a density dependent loss term for phytoplankton S_{POC} is the sinking rate of POC and all others as above.

Table 10: List of Parameters used in bacterial remineralisation of POC

Term	Variable	Description	Where set
K_P	rn_mokpft	half saturation constant for mortality	*namelist.trc.sms*
POC_{riv}	deppoc	river input of POC_s	*trcini.dgom.h*
S_{POC}	rn_snkpoc	sinking speed of POC	*namelist.trc.sms*

5.5 Large particulate organic carbon - GOC

The temporal derivative of large POC (GOC) is calculated as

$$\frac{\partial GOC}{\partial t} = \underbrace{\sum_j \xi^{Z_j} \sum_k g^{Z_j}_{F_k} * Z_j * F_k}_{zooplankton\ unassimilated\ food} - \underbrace{\sum_j g^{Z_j}_{GOC} * Z_j * GOC}_{loss\ through\ grazing} + \underbrace{\sum_j m^{Z_j}_{0^\circ} * c^T * Z_j}_{mortality}$$
$$+ \underbrace{\sum_i w^{P_i}_{agg} {P_i}^2}_{phytoplankton\ aggregation} + \underbrace{\Phi^{DOC\to GOC}_{agg} + \Phi^{POC\to GOC}_{agg}}_{aggregation\ to\ GOC}$$
$$- \underbrace{\lambda^{\star}_{GOC} GOC}_{GOC\ dissolution} - \underbrace{V_{sink} \frac{\partial GOC}{\partial z}}_{GOC sinking}. \tag{43}$$

ξ^{Z_j} is unassimilated fraction of material grazed by meso- and macro-zooplankton and m^{Z_j} is meso- and macro-zooplankton mortality as in equation (17). In PlankTOM5 only the meso-zooplankton contributions are considered. $w^{P_i}_{agg}$ is an aggregation constant for density dependent loss by silicifiers (diatoms) and N_2 fixers; in PlankTOM5 only the loss by silicifiers is considered. V_{sink} is the sinking rate of GOC and is calcuated as equation 41.

Chapter 6

Carbonate chemistry

6.1 Calcite - CAL

Calcification in the model is performed only by phytoplankton calcifiers, COC. Losses of calcifiers result in detached/sinking $CaCO_3$, and enters the tracer CAL. Attached $CaCO_3$ is produced in a fixed ratio to organic matter and therefore there is no tracer for its concentration. It does however reduces alkalinity, ALK, and dissolved inorganic carbon, DIC. The source and sinks for detached carbonate (CAL), dissolved inorganic carbon (DIC) and alkalinity (ALK) are shown in Figure 6

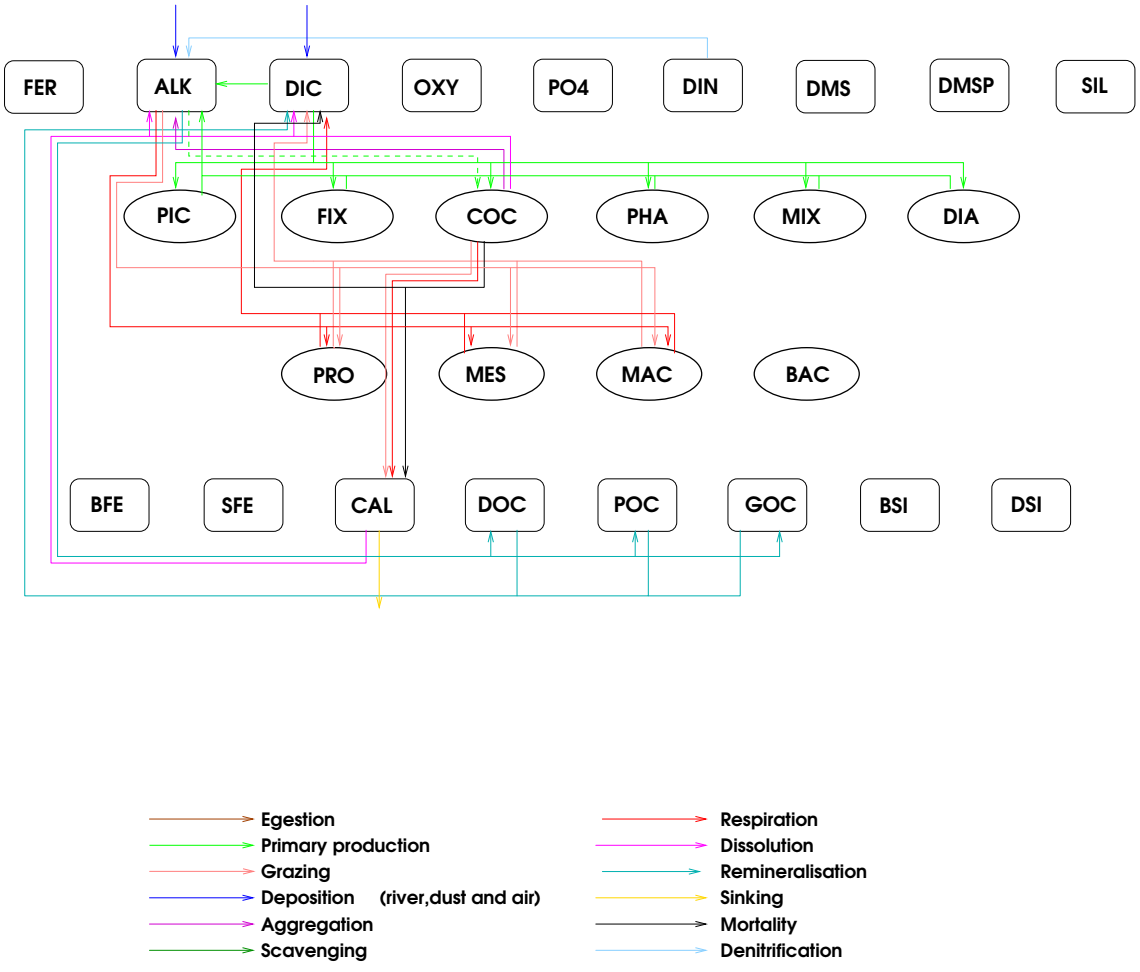

Figure 6: The source and sinks for detached carbonate (CAL), dissolved inorganic carbon (DIC) and alkalinity (ALK).

$$\frac{\partial CaCO_{3attached}}{\partial t} = R_{cal}\Bigg(\underbrace{(1-\delta^{COC})\mu^{COC}COC}_{production\ by\ COC} - \underbrace{m^{COC}\frac{COC}{K_{COC}+COC}COC}_{COC\ mortality} - \underbrace{w_{agg}^{COC}COC^2}_{COC\ respiration} - \underbrace{\sum_j g_{Z^j}^{COC} * Z_j * COC}_{grazing\ by\ zooplankton}\Bigg) \quad (44)$$

For detached $CaCO_3$, CAL:

$$\frac{\partial CAL}{\partial t} = R_{cal}(1-R_{diss})\Bigg(\underbrace{m^{COC}\frac{COC}{K_{COC}+COC}COC}_{COC\ mortality} + \underbrace{w_{agg}^{COC}COC^2}_{COC\ respiration} + \underbrace{\sum_j g_{COC}^{Z_j} Z_j * COC}_{grazing\ by\ zooplankton}\Bigg) - \underbrace{V_{sink}\frac{\partial CAL}{\partial z}}_{sinking} - \underbrace{\lambda_{CO_3} CaCO_3}_{dissolution}, \quad (45)$$

where R_{cal} is the calcification to particulate primary production ratio, R_{diss} is the fraction of attached coccoliths that is dissolved during losses of coccolithophores, V_{sink} is the sinking speed and is described in section 5.3, and λ_{CO_3} is the dissolution rate:

$$\lambda_{CO_3} = MIN\left(1, \frac{1-\delta_{sat}}{K_{cal}+\delta_{sat}}\right) \quad (46)$$

where δ_{sat} is the deviation from saturation and K_{cal} is the half saturation constant for calcite dissolution. λ_{CO_3} is $0.25\ month^{-1}$ at the sea surface, and $1\ month^{-1}$ at and below saturation.

CAL is calculated in *bgcbio* and reduced by the fraction dissolved in *bgclys* .

Table 11: List of Parameters used in evolution of calcite

Term	**Variable**	**Description**	**Where set**
R_{cal}	rn_coccal	$CaCO_3$ to Carbon ratio	*namelist.trc.sms*
δ^{coc}	rn_docphy	excretion ration for coccolithophorids	*namelist.trc.sms*
$\mu^{COC}COC$	prophy	coccolithophorid productivity	*bgcpro*
$m^{COC}\frac{COC}{K_{coc}+COC}COC$	torphy	coccolithophorid mortality	*bgclos*
$w_{agg}^{coc}COC^2$	resphy	coccolithophorid respiration	*bgcnul,bgcsnk*
R_{diss}	rn_discal	Fraction of $CaCO_3$ dissolved during coccolithophorid death	*namelist.trc.sms*
K_{cal}	rn_lyscal	half saturation constant for calcite dissolution	*namelist.trc.sms*
δ_{sat}	delco3	deviation from saturation	*bgclys*
$\lambda_{CO_3}CaCO_3$	remco3	dissolved $CaCO_3$	*bgclys*
V_{sink}	xvsink	sinking speed of $CaCO_3$	*bgcsnk*
	sinkcal	sinking $CaCO_3$ at depth z	*bgcsnk*

6.2 Dissolved inorganic carbon - DIC

The temporal evolution of dissolved inorganic carbon, DIC, is calculated as:

$$\begin{aligned}\frac{\partial DIC}{\partial t} &= \underbrace{-\sum_i \mu^{P_i} P_i}_{primary\ production} + \underbrace{consum}_{respiration} - \underbrace{R_{cal}(1-\delta^{COC})\mu^{COC} COC}_{attached\ CaCO_3} \\ &+ \underbrace{R_{diss}(m^{COC}\frac{COC}{K_{COC}+COC}COC + w_{agg}^{COC} COC^2 + \sum_j g_{COC}^{Z_j} Z_j COC)}_{dissolved\ COC} \\ &+ \underbrace{DIC_{riv}}_{river\ depostion} + \underbrace{\lambda_{CO_3} CaCO_3}_{dissolution} + \underbrace{F_{air-sea}^{CO_2}}_{air-sea\ flux} . \end{aligned} \quad (47)$$

In PlankTOM5 $consum$ includes the fraction of grazing by micro and meso-zooplankton that goes to inorganic carbon and the fraction of DOC, POC and GOC which is remineralised.

In PlankTOM10 in addition to the inclusion of grazing by macro-zooplankton remineralistion by bacteria is included as a function of their growth efficiency and respiration:

$$\begin{aligned} consum &= \underbrace{\sum_j \sigma^{Z_j} * (1 - \xi^{Z_j} - MGE^{Z_j}) \sum_k g_{F_k}^{Z_j} * Z_j * F_k}_{grazing} \\ &+ \underbrace{(1-BGE) * (\lambda_{DOC}^{\star} DOC + \lambda_{POC}^{\star} POC + \lambda_{GOC}^{\star} GOC)}_{remineralisation} \\ &+ \underbrace{\sum_j R_{0^\circ}^{Z_j} d^T * Z_j}_{respiration} . \end{aligned} \quad (48)$$

where the sum over j includes both the zooplankton and bacteria. The bacterial growth efficiency, BGE, is given by Equation 24. The terms for attached $CaCO_3$ and production of DIC by dissolution are described in Section 6.1. River deposition DIC_{riv} is the input of DIC from rivers, see Section 11.6. The air-to-sea flux is described in Chapter 10..

Dissolved inorganic carbon is calculated in *bgcbio* ; in *bgclys* the $CaCO_3$ dissolution to DIC is included while in *bgcflx* the air-sea flux of DIC is added.

Table 12: List of Parameters used in the evolution of DIC and ALK

Term	Variable	Description	Where set
MGE^{bac}	bactge	bacteria growth efficiency	*bgcbio,bgcsnk*
$R_{0^\circ}^{bac}$	rn_resbac	respiration of bacteria at 0°C	*namelist.trc.sms*
$depdic$		river input of DIC	*river.nc*
GGE^{bac}	rn_ggebac	gross growth efficiency of bacteria	*namelist.trc.sms*
$R_{\frac{N}{C}}$	alknut	N+S+P to Carbon ratio	*trcini.dgmo.h90*
DIC_{riv}	depdic	River deposition of DIC	*trcini.dgom.h90*

6.3 Alkalinity - ALK

The temporal evolution of alkalinity is calculated as:

$$\begin{aligned}\frac{\partial ALK}{\partial t} &= \underbrace{R_{\frac{N}{C}}\big(\sum_i \mu^{P_i} P_i - \sum_j consum^{Z_j} Z_j\big)}_{inorganic\ to\ organic\ C\ conversion} - \underbrace{2 * R_{cal}(1-\delta^{coc})\mu^{coc} COC}_{removal\ of\ CO_3^{2'}\ by COC} \\ &+ \underbrace{2 * R_{cal} * R_{diss}\big(m^{coc}\frac{COC}{K_{coc}+COC}COC + w_{agg}^{coc} COC^2 + \sum_j g_{coc}^{Z_j} * Z_j * COC\big)}_{production\ of\ CO_3^{2'}\ by\ COC\ dissolution} \\ &+ \underbrace{DIC_{riv}}_{river\ deposition} + \underbrace{N_{denit}}_{denitrification} + \underbrace{2 * \lambda_{CO_3} CaCO_3}_{dissolution\ of\ CaCO_3} \end{aligned} \quad (49)$$

where $R_{\frac{N}{C}} = \frac{N+S+P}{C}$ is the effect of nutrient uptake and remineralisation on alkalinity (Wolf-Gladrow et al., 2007). The terms for the production of attached $CaCO_3$, dissolved COC and dissolved $CaCO_3$ are described in Section 6.1. River deposition, DIC_{riv} is described in Section 11.6 and denitrification, N_{denit} in Section 7.3.

Chapter 7

Nutrients and Oxygen

The processes governing the evolution of dissolved iron (FER),large (BFE) and small (SFE) particulate iron, dissolved silica (SIL), biogenic silica (BSI) and detrital silica (DSI) are shown in Figure 7.

The processes governing the evolution of phosphate (PO4), dissolved inorganic nitrogen (DIN) and oxygen (OXY) are shown in Figure 8.

7.1 The Iron Cycle

7.1.1 Fe in PFTs

The iron content of phytoplankton (DFE for silicifiers, NFE for mixed-phytoplankton, CFE for calcifiers, PFE for picophytoplankton, HFE for DMSp and FFE for N_2-fixers) is currently being adapted. The previous version is a steady state solution to the Geider et al. (1996) model.

$$\begin{aligned}\frac{\partial Fe^{P_i}}{\partial t} &= \underbrace{(1-\delta^{P_i})\rho_{Fe}^{P_i}\mu^{P_i}P_i^2 * \frac{FER}{K_{FER}^{P_i}+FER}}_{production} - \underbrace{m^{P_i}\frac{P_i^2}{K_P+P_i} * \frac{Fe^{P_i}}{P_i}}_{mortality} \\ &- \underbrace{w_{agg}^{P_i}P_i^2 * \frac{Fe^{P_i}}{P_i}}_{aggregation\ loss} - \underbrace{\sum_j g_{P_i}^{Z_j}Z_jP_i * \frac{Fe^{P_i}}{P_i}}_{grazing\ loss} \end{aligned} \tag{50}$$

where FER is the dissolved iron, $K_{FER}^{P_i}$ is the half saturation constant for Fe for phytoplankton P_i and:

$$\rho_{Fe}^{P_i} = \frac{15*10^{-6}}{.6*b^T*2*10^5*\alpha^{P_i}*P_i} \tag{51}$$

$$\tag{52}$$

See also Section 3.3 of the Supplement to Aumont and Bopp (2006a). The new version is a dynamical photosynthesis model (Buitenhuis and Geider, in prep.). The Fe/C ratio of zooplankton is fixed. If zooplankton graze on phytoplankton that have a higher Fe:C ratio than themselves, the excess is remineralised to dissolved iron. If the phytoplankton Fe/C ratio is lower than zooplankton Fe:C, the model growth efficiency (MGE) is decreased:

$$MGE^{Z_j} = MIN\left(1-\xi^{Z_j}, \sum_k \frac{g_{F_k}^{Z_j} * \frac{Fe_{F_k}}{F_k} * (1-\xi^{Z_j})}{MAX\left(g_{F_k}^{Z_j} * \left(\frac{Fe}{C}\right)_Z, 1e-25\right)}\right) \tag{53}$$

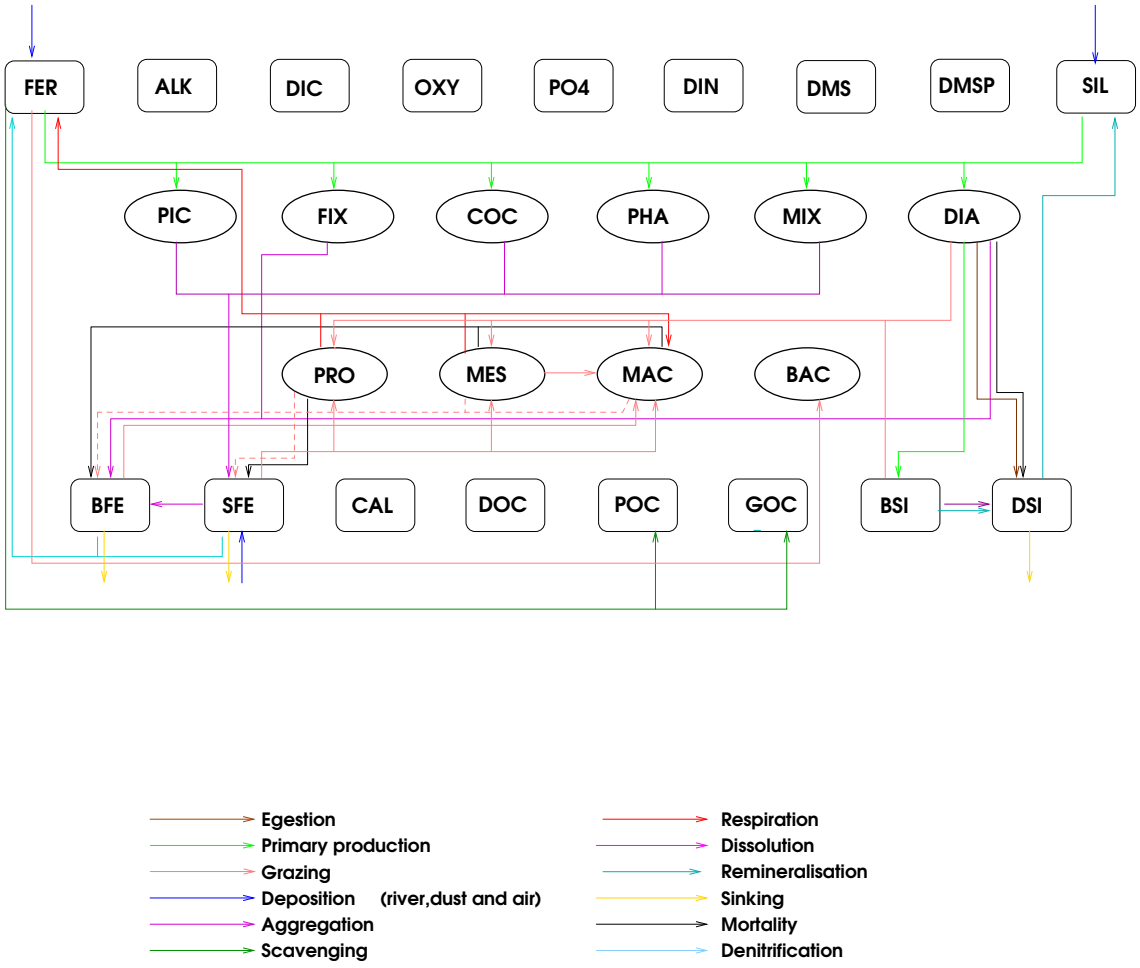

Figure 7: The source and sinks for dissolved iron (FER), large (BFE) and small (SFE) particulate iron, dissolved silica (SIL, biogenic silica (BSI) and detrital silica (DSI).

7.1.2 Fe in detrital matter - BFE, SFE

Iron in detrital matter is divided into BFE in large organic particles (GOC) and SFE in small organic particles POC. Production terms of particulate organic iron follow the Fe/C ratio of the source organisms. There is no iron in DOM, but iron is added from dissolved iron to particulate organic iron during degradation of DOM. Degradation of POM conserves the Fe:C ratio of POM. The bottom correction removes as much carbon from the bottom water layers as is added by rivers. Because iron is scavenged, the Fe/C ratio of POM sometimes becomes excessive. It is therefore set to a maximum, currently 10^{-3} mol:mol.

$$\begin{aligned}\frac{\partial BFE}{\partial t} &= \underbrace{\sum_{i=DIA,FIX} \omega_{agg}^{P_i} P_i^2}_{aggregation} - \underbrace{\sum_j g_{GOC}^{Z_j} * Z_j * GOC \frac{BFE}{GOC}}_{grazing\ loss} + \underbrace{\sum_{j=MES,MAC} \xi^{Z_j} \sum_k g_{F_k}^{Z_j} * Z_j * F_k \frac{Fe_{F_k}}{F_k}}_{unassimilated\ food} \\ &+ \underbrace{\left(\frac{Fe}{C}\right)_Z \sum_{j=MES,MAC} m_0^{Z_j} c_{Z_j}^T * Z_j}_{mortality} + \underbrace{\phi_{agg}^{POC \to GOC} \frac{SFE}{POC}}_{Fe\ aggregation} - \underbrace{\lambda_{GOC}^* Fe}_{remineralisation} \\ &- \underbrace{V_{sink} \frac{\partial BFE}{\partial z}}_{sinking\ of\ BFE} \end{aligned} \tag{54}$$

$$\begin{aligned}\frac{\partial SFE}{\partial t} &= \underbrace{\sum_{i=PIC,MIC,COC,PHA} \omega_{agg}^{P_i} P_i^2}_{aggregation} - \underbrace{\sum_j g_{POC}^{Z_j} * Z_j * POC \frac{SFE}{POC}}_{grazing\ loss} + \underbrace{\xi^{MIC} \sum_k g_{F_k}^{MIC} * MIC * F_k \frac{Fe_{F_k}}{F_k}}_{unassimilated\ food} \\ &+ \underbrace{\left(\frac{Fe}{C}\right)_Z m_0^{MIC} c_{MIC}^T * MIC}_{mortality} - \underbrace{\phi_{agg}^{POC \to GOC} \frac{SFE}{POC}}_{Fe\ aggregation} - \underbrace{\lambda_{POC}^* Fe}_{remineralisation} \\ &- \underbrace{S_{POC} \frac{\partial SFE}{\partial z}}_{sinking\ of\ SFE} + \underbrace{\left(\frac{Fe}{C}\right)_Z POC_{riv}}_{river\ deposition} \end{aligned} \tag{55}$$

7.1.3 Dissolved Fe - FER

The temporal evolution of dissolved iron, FER, is calculated as follows:

$$\begin{aligned}\frac{\partial FER}{\partial t} &= \underbrace{\sum_i (1 - \delta^{P_i}) \mu^{P_i} P_i}_{loss\ through\ phytoplankton\ productivitiy} + \underbrace{\left(\frac{Fe}{C}\right)_Z \sum_j R_0^{Z_j} d_{Z_j}^T}_{respiration} \\ &+ \underbrace{\sum_j \left(\sum_k g_{f_k}^{z_j} * Z_j * F_k \frac{Fe}{F_k} (1 - \xi^{Z_j}) - \left(\frac{Fe}{C}\right)_Z \sum_k g_{F_k}^{Z_j} * Z_j * F_k * MGE^{Z_j} \right)}_{grazing\ loss} \\ &+ \underbrace{FER_{remin}}_{FER\ from\ remineralisation} - \underbrace{FER_{bac}}_{bacterial\ demand\ for\ FER} \\ &- \underbrace{Fe_{scav}}_{scavenging} + \underbrace{Fe_{dep}}_{dust\ deposition} + \underbrace{Fe_{riv}}_{river\ deposition} \end{aligned} \tag{56}$$

Iron is input from rivers, see Section 11.6, and the dissolution of dust from the atmosphere, see Section 11.5. Iron is taken up by phytoplankton during primary production (see above).

When iron concentration is above 0.6 nM, it is scavenged by POM: the evolution of scavenged iron,

Fe_{scav} is calculated as:

$$\begin{aligned}\frac{\partial Fe_{scav}}{\partial t} &= k_{sc} * ((POC + GOC) * 1e6)^{0.6} \\ &* \frac{-(1 + Fe_{par} * k_{eq}) + ((1 + Fe_{par} * k_{eq})^2 + 4 * FER * k_{eq})^{0.5})}{2 * k_{eq}}\end{aligned} \tag{57}$$

where Fe_{par} = ($0.6 * 10^{-9} - FER$), k_{sc} is the scavenging rate (= 0.01 d^{-1}) and k_{eq} = 1.2*10^{13}. The scavenged iron is not added to POM, but removed from the model.

Bacteria demand for Fe can be supplied from the remineralisation of BFE and SFE and from dissolved iron. The net effect on FER may be an increase - if remineralisation exceeds the bacterial demand or a decrease if demand exceeds that supplied by remineralisation. Bacterial demand for FER, FER_{bac} is:

$$FER_{bac} = \frac{BGE\left(\frac{Fe}{C}\right)_Z * (\lambda^*_{DOC}DOC + \lambda^*_{POC}POC + \lambda^*_{GOC}GOC - \lambda^*_{POC}Fe - \lambda^*_{GOC}Fe)FER}{K^{bac}_{FER} + FER} \tag{58}$$

or zero if this is negative.
The contribution to FER from remineralisation of BDE and SFE is:

$$FER_{remin} = -BGE\left(\frac{Fe}{C}\right)_Z * (\lambda^*_{DOC}DOC + \lambda^*_{POC}POC + \lambda^*_{GOC}GOC - \lambda^*_{POC}Fe - \lambda^*_{GOC}Fe) \tag{59}$$

or zero if this is negative.

Table 13: List of Parameters used in evolution of iron

Term	Variable	Description	Where set
FER_{remin}	rbafer	Dissolved from remineralisation of organic detrital Fe	*bgcsnk*
Fe_{scav}	xscave	Iron scavenged by particualte organic matter	*bgcsnk*
Fe_{riv}	depfer	River deposition	*trcini.dgom.h90*
Fe_{dep}	irondep	Dust deposition	
k_{sc}	rn_scofer	Scavenging rate	*namelist.trc.sms*
k_{eq}	xkeq	Scavenging rate parameter = 1.2e13	*bgcsnk*

7.2 The Silicate cycle

Silica is input from rivers and the dissolution of dust from the atmosphere. Growth of diatoms consumes dissolved silica (SIL) from the water to produce hydrated silica (biogenic silica BSI). Loss processes of diatoms produce sinking particulate silica (DSI).

7.2.1 Dissolved SiO_3 - SIL

The temporal evolution of dissolved silica is calculated as:

$$\begin{aligned}\frac{\partial SIL}{\partial t} &= \underbrace{-0.15\mu_{DIA} * DIA \min\left(1, \frac{SIL}{K_{Si}}\right)\left(\frac{Si}{C}\right)_{DIA}}_{production\ of\ BSI\ by\ diatoms} + \underbrace{\lambda_{Si}DSI}_{remineralisation\ of\ sinking\ silica} \\ &+ \underbrace{SIL_{riv}}_{river\ input} + \underbrace{SIL_{dep}}_{atmospheric\ input}\end{aligned} \tag{60}$$

where$\mu_{DIA} * DIA$ is the primary production, in terms of carbon, of diatoms, K_{Si} is the half saturation constant for SiO_3 in diatoms, λ_{Si} is the remineralisation rate of silica which is dependent on temperature, T and oxygen OXY:

$$\lambda_{Si} = \min\left(1.2 * 10^{16} e^{\frac{-11200}{(273.15+T)}}, .1\right)\eta_O. \tag{61}$$

$\left(\frac{Si}{C}\right)_{DIA}$ increases with iron stress and silicate availability:

$$\left(\frac{Si}{C}\right)_{DIA} = 4. - 3 * min\left(\frac{max(0, FER)}{K_{SIL}^{DIA}}, 1\right). \tag{62}$$

Observations in the Southern Ocean show a high $\left(\frac{Si}{C}\right)_{DIA}$ ratio in areas with very high Si concentration so $\left(\frac{Si}{C}\right)_{DIA}$ is arbitrarily increased throuhout the ocean to reflect this:

$$\left(\frac{Si}{C}\right)_{DIA} = \frac{6. * SIL}{SIL + K_{BSI}}. \tag{63}$$

Table 14: List of Parameters used in evolution of silica

Term	Variable	Description	Where set
$\lambda_{Si} SIL$	siremin	remineraliation rate of silica	*bgcsnk*
$\mu_{DIA} DIA$	prophy(1)	primary production, in terms of carbon,of diatoms	*bgcpro bgcnul*
K_{SIL}^{DIA}	rn_sildia	half saturation constant for SiO_3 in diatoms	*namelist.trc.sms*
$\left(\frac{Si}{C}\right)_{DIA}$	silfac	Si/C ratio of diatoms	*bgcpro*
K_{BSI}	rn_kmsbsi	half saturation constant for $\left(\frac{Si}{C}\right)$	*namelist.trc.sms*
SIL_{riv}	depsil	river input of SiO_3	*trcini.dgom.h90*
SIL_{atm}	sidep	input of atmospheric silica to the water column	*bgcbio*
δ^{DIA}	rn_docphy	scretion ratio for diatoms	*namelist.trc.sms*

7.2.2 Biogenic particulate silica - BSI

The temporal evolution of biogenic silica is calculated as:

$$\begin{aligned} \frac{\partial BSI}{\partial t} &= \underbrace{0.15 \mu_{DIA} DIA \min\left(1, \frac{SIL}{K_{SIL}}\right)\left(\frac{Si}{C}\right)_{DIA}(1 - \delta^{DIA})}_{production\ by\ diatoms} \\ &- \underbrace{\sum_j g_{DIA}^{Z_j} * DIA \frac{BSI}{DIA}}_{grazing} - \underbrace{m^{DIA} \frac{BSI}{(K_{DIA} + DIA)} * DIA}_{remineralisation\ due\ to\ diatom\ mortality} \\ &- \underbrace{w_{agg}^{DIA} \frac{BSI}{DIA}}_{sinking\ of\ excreted\ silica} \end{aligned} \tag{64}$$

where δ^{DIA} is the excretion ratio for diatoms.

7.2.3 Sinking particulate silica - DSI

The temporal evolution of sinking particulate silica is calculated as:

$$\begin{aligned} \frac{\partial DSI}{\partial t} &= \underbrace{0.15 \mu_{DIA} DIA \min\left(1, \frac{SIL}{K_{SIL}}\right)\left(\frac{Si}{C}\right)_{DIA}}_{diatom\ excretion} + \underbrace{m^{DIA} \frac{BSI}{(K_P + DIA)} * DIA}_{remineralisation\ due\ to\ diatom\ mortality} \\ &+ \underbrace{\sum_j g_{DIA}^{Z_j} * DIA \frac{BSI}{DIA}}_{grazing} + \underbrace{w_{agg}^{DIA} \frac{BSI}{DIA}}_{sinking\ of\ excretedsilica} - \underbrace{\lambda_{Si} DSI}_{remineralistion\ of\ BSI} \\ &+ \underbrace{\omega^{GOC} \frac{\partial DSI}{\partial z}}_{sedimentation\ of\ DSI\ in\ GOC} \end{aligned} \tag{65}$$

where δ^{DIA} is the excretion ratio for diatoms as above.

7.3 Phosphorus and Nitrogen - PO4 and DIN

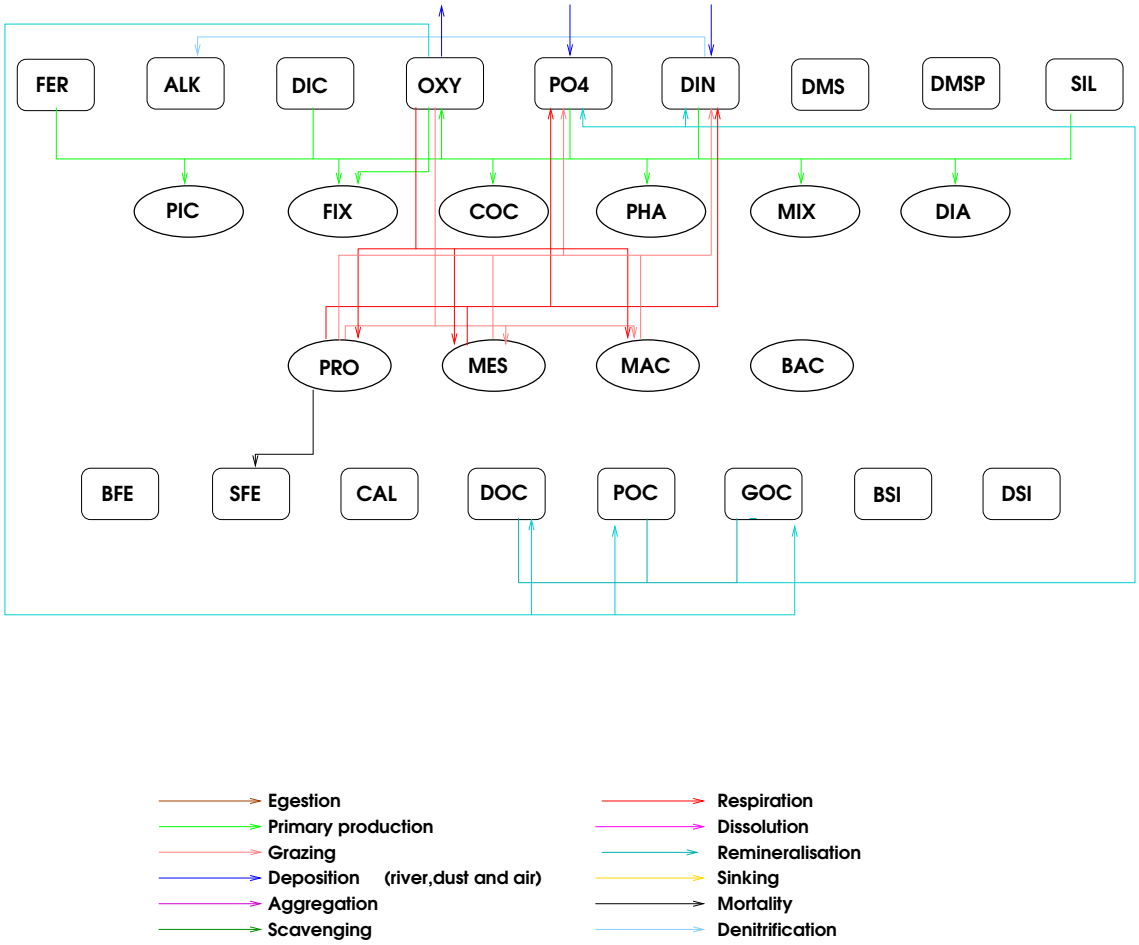

Figure 8: The source and sinks for phophate (PO4), nitrogen (DIN) and oxygen (OXY).

Phosphate is input to the ocean by river deposition; it is consumed during phytoplankton growth and produced during respiration.

$$\frac{\partial PO4}{\partial t} = \underbrace{-\sum \mu^{P_i} P_i}_{production} + \underbrace{consum}_{respiration\ and\ remineralisation} + \underbrace{PO4_{riv}}_{river\ deposition} \tag{66}$$

where $consum$ is described in Section 6.2 and defined in equation 48

In PlankTOM5 nitrate and phosphate are linked through a constant Redfield ratio. The concentration of P is represented in C equivalent, wher 1mol of P in the model is equal to 122 mol. Thus to compare model P to observations (in molP/l) the model P must be divided by 122.

$$\frac{\partial PO4}{\partial t} = \underbrace{-\sum \mu^{P_i} P_i}_{production} + \underbrace{\sum consum^{Z_i} Z_i}_{respiration\ and\ remineralisation} + \underbrace{PO4_{riv} + NO3_{riv}}_{river\ deposition} - \underbrace{N_{denit}}_{loss\ through\ denitrifcation} \quad (67)$$

where

$$N_{denit} = 0.8 \left(\frac{O}{C} consum * resp_{bac}^{NO_3} \right), \quad (68)$$

where $resp_{bac}^{NO_3}$ is the fraction of bacterial respiration that uses NO_3 rather than O_2 and is described in Section 7.4.

In PlankTOM10 Dissolved inorganic nitrogen is a separate tracer:

$$\frac{\partial DIN}{\partial t} = \underbrace{-\sum \mu^{P_i} P_i \frac{N}{C} DIN_{nit}}_{phytoplanktonproduction} + \underbrace{consum \frac{N}{C}}_{respiration\ and\ remineralistation} - \underbrace{N_{denit}}_{denitrification} + \underbrace{DIN_{riv}}_{river\ input} . \quad (69)$$

In this equation DIN_{nit} is 1 for all phytoplankton type except for N_2 fixers for which it represents the nitrate limited fraction of growth on NO_3 rather than N_2:

$$DIN_{nit} = \frac{\frac{DIN}{DIN + K_{NO_3}^{fix}}}{\frac{DIN}{DIN + K_{NO_3}^{fix}} + R_{fix} \left(1 - \frac{DIN}{DIN + K_{NO_3}^{fix}} \right)}. \quad (70)$$

Table 15: List of Parameters used in the evolution of phosphate and nitrogen

Term	Variable	Description	Where set
N_{denit}	denitr	denitrification	*bgcbio*
$PO4_{riv}$	deppo4	River input of phosphate in mole	*trcini.dgom*
$NO3_{riv}$	depnit	River input of NO_3	*trcini.dgom*
K_{NO_3}	rn_kmnphy	NO_3 half saturation constants for phytoplankton	*namelist.trc.sms*
R_{fix}	rn_munfix	Fraction of growth rate during N_2 fixation relative to growth on NO_3	*namelist.trc.sms*
DIN_{nit}	dinpft	fraction of phyto growth that is supported by NO_3 rather than N_2	*bgcpro*
$resp_{bac}^{NO_3}$	nitrfac	fraction of bacterial respiration using NO_3 rather than O_2	*bgcnul*

7.4 Oxygen - OXY

Oxygen is produced during the growth of phytoplankton. It is consumed during the growth of N_2 fixers on N_2 and during the remineralisation described by the term $consum$ in Section 6.2. There is also an exchange

of oxygen with the atmosphere.

$$\begin{aligned}\frac{\partial OXY}{\partial t} &= \underbrace{\frac{O}{C}\sum \mu^{P_i} P_i}_{phytoplankton\ growth} - \underbrace{\frac{N}{C}\mu^{P_{fix}} P_{fix} 1.25(1 - DIN_{nit})}_{growth\ of\ N_2\ fixers\ on N_2} \\ &- \underbrace{\frac{O}{C} consum(1 - resp_{bac}^{NO_3})}_{remineralisation} + \underbrace{F_{air-sea}^{O_2}}_{O_2\ flux\ from\ air\ to\ sea}\end{aligned} \tag{71}$$

The fraction of bacterial respiration that uses NO_3 rather than O_2, $resp_{bac}^{NO_3}$ is given by:

$$resp_{bac}^{NO_3} = \frac{\sin\left(\max\left(-.5, \frac{10E-6-OXY}{20E-6+OXY}\right) * \pi\right) + 1}{2} \tag{72}$$

The air-sea exchange of oxygen, $F_{air-sea}^{O_2}$, is calculated in *bgcflx* and described in 10.2.

Chapter 8

Isotopes

8.1 ^{18}O -O18

$$\begin{aligned}\frac{\partial O18}{\partial t} &= \text{phytoplankton growth} - \text{remineralisation} + \text{air-ocean flux} \\ &= \frac{O}{C}\Sigma\mu^{P_i}P_i{}^{18}O^{phy}_{frn} - \frac{O}{C}consum(1-resp^{NO_3}_{bac})^{18}O^{bac}_{frn} * \frac{O18}{OXY} \\ &+ {}^{18}O_{air-sea}. \end{aligned} \tag{73}$$

The fractionation of ^{18}O during photosynthesis, $^{18}O^{phy}_{frn}$, is dependent on the salinity and is calculated in *bgcbio* from:

$$^{18}O^{phy}_{frn} = \left(0.5\frac{(sal-34.8)}{1000}+1\right)2005.16*10^{-6} \tag{74}$$

Table 16: List of Parameters used in the evolution of ^{18}O

Term	Variable	Description	Where set
$^{18}O^{bac}_{frn}$	rn_fac018	Bacterial fractionation for ^{18}O	namelist.trc.sms
$^{18}O^{phy}_{frn}$	bacfra	Fractionation of ^{18}O during photosynthesis	*bgcbio*
sal	sn	salinity	

8.2 ^{13}C - 13C

The evolution of ^{13}C is calcuated in *bgcflx* and *bgclys* .

$$\begin{aligned}\frac{\partial 13C}{\partial t} &= \text{air-ocean flux} - \text{ocean-air flux} + \text{dissoluton of } CaCO_3 \\ &= CO_{2_{air-sea}}\left(\frac{^{13}C}{^{12}C}\right)_{air} CO^{sea}_{2_{frn}} - CO_2 sea - air\left(\frac{^{13}C}{^{12}C}\right)_{sea} CO^{air}_{2_{frn}} \\ &- \lambda_{CO_3} CaCO_3 \left(\frac{^{13}C}{^{12}C}\right)_{PDB}. \end{aligned} \tag{75}$$

The calculation of the flux terms $CO_{2_{air-sea}}$ and $CO_{2_{sea-air}}$ is described in Section 10.1.

Table 17: List of Parameters used in the evolution of ^{13}C

Term	Variable	Description	Where set
$CO_{2_{air-sea}}$	fld	air to sea flux of CO_2	*bgcflx*
$\left(\frac{^{13}C}{^{12}C}\right)_{air}$	rela13	^{13}C to ^{12}C ratio in air	*bgcflx*
$CO^{sea}_{2_{frn}}$	frw13	^{13}C fractionation in water	*bgcflx*
$CO_{2_{sea-air}}$	flu	sea to air flux of CO_2	*bgcflx*
$\left(\frac{^{13}C}{^{12}C}\right)_{sea}$	relw13	^{13}C to ^{12}C ratio in surface water	*bgcflx*
$CO^{air}_{2_{frn}}$	fra13	^{13}C fractionation in air	*bgcflx*
$\left(\frac{^{13}C}{^{12}C}\right)_{PDB}$	pdb	^{13}C fractionation in standard belemnite	*trcini.dgom*

Chapter 9

Sulphur cycling

9.1 DMSP and DMS

9.1.1 Description and modelled tracers

Dimethylsulphide (DMS) is a marine biogenic trace gas produced in planktonic food webs from its precursor dimethylsulphoniopropionate (DMSP). DMS is thought to be involved in cloud formation processes through the oxidation of DMS transferred across the sea-air interface. Oxidation products of DMS can form sulphate aerosol and may lead to the formation of new cloud condensation nuclei (CCN). Hence, changes in the sea-air flux of DMS may alter cloud cover and may affect the global albedo.

The DMS cycle is described by three additional variables: dimethylsulphide (DMS), particulate dimethylsulphoniopropionate (DMSPp) and dissolved DMSP (DMSPd). All equations are semi-empirical and take into account current experimental constraints on the parameters used. Within the range of parameter uncertainty, the model has been tuned to optimise the representation of DMS seasonality. The sulphur mass budget is not closed and sulphur is never limiting to DMSP synthesis by phytoplankton.

9.1.2 Temporal evolution of the tracer

Dynamics of DMSPp, DMSPd and DMS

The dynamics of DMS, DMSPp and DMSPd are described according to the following equations:

$$DMSPp(t) = \underbrace{\sum_i q_i(t) * P_i(t)}_{phytoplankton\ production} \tag{76}$$

$$\begin{aligned} \frac{\partial DMSPd}{\partial t} &= \underbrace{\sum_i \left[(1-\alpha_{dms}) * \left(\sum_j \lambda_{m_g}^{Z_j} * g_{P_i}^{Z_j} + m_{P_i} \frac{P_i}{K_{P_i}+P_i} \right) * q_i(t) \right]}_{production\ through\ zooplankton\ grazing\ and\ mortality} \\ &- \underbrace{\lambda^{DL} * DMSPd}_{removal\ through\ cleavage} - \underbrace{\phi_{DMSP}^{bac} * DMSPd}_{bacterial\ degradation} \end{aligned} \tag{77}$$

$$\begin{aligned} \frac{\partial DMS}{\partial t} &= \underbrace{\sum_i \left[\alpha_{dms} * \left(\sum_j \lambda_{m_g}^{Z_j} * g_{P_i}^{Z_j} + m_{P_i} \frac{P_i}{K_{P_i}+P_i} + \lambda_{exud_i} * \frac{PAR}{PAR_{max}} * P_i \right) * q_i(t) \right]}_{production\ through\ zooplankton\ grazing,\ mortality\ and\ exudation} \\ &+ \underbrace{\mu^{bac} * \phi_{DMSP}^{bac} * DMSPd}_{bacterial\ production} + \underbrace{\lambda^{DL} * DMSPd}_{cleavage} \\ &- \underbrace{\lambda_{photo} * PAR * DMS}_{photolysis} - \underbrace{\phi_{DMS}^{bac} * DMS}_{bacterial\ degradation} - \underbrace{F_{sea-air}^{DMS}}_{sea\ to\ air\ flux} \end{aligned} \tag{78}$$

where q_i is the internal cell quota for DMSP, i denotes the different phytoplankton functional types and t is the time step. P_i is the phytoplankton concentration ($\frac{mol(C)}{L}$). The parameters λ, α, μ describe constant scaling parameters for grazing, cleavage by free DMSP-lyase, exudation and bacterial degradation, respectively. The functions ϕ describe functional dependencies that multiply with concentrations in order to yield rates for the sink terms. DMS and DMSP are released in zooplankton grazing ($\frac{mol(C)}{L\,t}$), bac described terms related to bacterial biomass ($\frac{mol(C)}{L}$) or activity. $DMSPp$ designates the DMSPp concentration ($\frac{mol(DMSPp)}{L}$), $DMSPd$ the DMSPd concentration ($\frac{mol(DMSPd)}{L}$) and DMS is the DMS concentration ($\frac{mol(DMS)}{L}$). F^{DMS} is the sea-to-air flux of DMS (Wanninkhof, 1992; Saltzman, 1993).

9.1.3 Source terms

The cell quota

The DMSPp cell quota of PFT i, q_i, describes the ratio of sulphur to carbon for each pPFT. In laboratory and field experiments, this quota has been observed to vary with algal taxon, species, and environmental conditions (temperature, nutrient status, solar radiation dose; reviewed e.g. in Stefels et al. 2007). Given the large differences in DMSPp quota between different species of the same algal taxon observed, and the large range of DMSPp levels observed within one species as a function of environmental stress, the cell quota of the pPFTs are only poorly restrained. Here, we assume a minimal cell quota q_{min}, using half the literature quota q_{lit} suggested in Stefels et al. (2007) for the modelled phytoplankton PFTs. The simulated cell quota is allowed to vary as a function of both light (PAR) and nutrient (Fe, PO_4) stress (Sunda et al., 2002) (s_1, s_2 and s_3) and is temperature (T) dependent. The T dependence simulates the function of DMS and DMSP in cryoprotection (Karsten et al., 1992, 1996). It has been set to only enhance the quota for temperatures of 0°C or below. All factors influencing the cell quota enter the equation for the cell quota multiplicatively.

Evaluating the resulting equation for q_i the quota has been set to vary between 0.8 $\times q_{min}$ and up to ca. 2.3 $\times$ the literature value (q_{lit}) (Stefels et al., 2007). Hence, the DMSP cell quota is described as:

$$q_i = \Big(\max(s_1, s_2, s_3) * 4. - f_{corr}\Big) * q_{min} * \Big(1 + \frac{1}{T + 2.5}\Big), \tag{79}$$

where

$$s_1 = \max\left(\frac{PAR}{PAR_{max}}, 0.3\right) \tag{80}$$

$$s_2 = \max\left(\frac{K^i_{Fe}}{Fe + K^i_{Fe}}, 0.3\right) \tag{81}$$

$$s_3 = \max\left(\frac{0.7 * K^i_{PO_4}}{PO_4 + K^i_{PO_4}}, 0.3\right) \tag{82}$$

$$q_{min} = \frac{1}{2} q_{lit}, \tag{83}$$

with an adjustable correction factor f_{corr} to tune global DMSPp concentrations, currently set to 0.5. Due to their definition, the environmental stressors s_1, s_2 and s_3 are dominant at different latitudes: while light stress is dominant in the low latitudes, PO_4 stress is greatest in temperate waters and Fe stress is maximal in the Southern Ocean (data not shown). Hence, light stress is expected to be most important for the simulation of the Summer Paradox.

Grazing, Mortality and Biomasses

The amount of biomass grazed per time step, $g^{Z_j}_{F_k}$ is described in equation 18. In the DMSP module, the ratio of DMSPd/DMS produced in grazing is described according to equations (77) and (78). α_{DMS} describes the ratio of DMS to DMSP released in grazing processes. It is assumed to be 1:9 (Archer et al., 2001). The constants $\lambda^Z_{m_g}$ have been defined in agreement with those for the cycling of carbon within the zooplankton grazers (Buitenhuis et al., 2006b). This means, that the fate of ingested DMSP is coupled to the fate of ingested carbon: in the model, a constant fraction of grazed carbon is incorporated into the

body mass of the grazers (e.g. 26%), a constant fraction is released to the water column due to 'sloppy feeding' (e.g. 11%), a constant fraction is respired (e.g. 33%) and the remaining ingested carbon is excreted into the seawater (e.g.30%) in zooplankton fecal material. Typical percentages are given but all may be set in *namelist.trc.sms.* With respect to DMSP, we assume that only the fraction incorporated into zooplankton biomass and parts of DMSP contained in fecal material is unavailable for further cycling. For the sake of simplicity we assume that all DMSPp contained in proto-zooplankton feces is part of the dissolved phase. Hence:

$$\lambda_{m_g}^{mic} = (1 - MGE^{mic}) \tag{84}$$

Using the above figures a total 74% of the DMSPp ingested by proto-zooplankton is released to the liquid phase as DMSPd and is available for further biological processing (Buitenhuis et al., 2006b). For meso-zooplankton:

$$\lambda_{m_g}^{mic} = (1 - MGE^{mes} - \beta_{mes} * \xi^{mes}) \tag{85}$$

where β_{mes} is the percentage of the DMSPp contained in the meso-zooplankton fecal pellets.

Exudation/Leakage

In response to the issues in Vézina et al. (submitted[1]) and based on the findings of Vallina et al. (2008) a term leading directly from phytoplankton to DMS as a function of environmental conditions has been implemented in this model. We call this term the "exudation term", despite the current lack of experimental evidence for such direct transfer of DMS across the cell membrane. The direct release of DMS from phytoplanktonic cells is in agreement with Sunda et al. (2002), i.e DMS may be part of an oxidant chain, produced under light and nutrient stress. The modelled exudation of DMS is assumed to be light dependent and proportional to the intracellular DMS(P) concentration. The exudation rates are a factor 4 lower than those used in Vallina et al. (2008) and vary with phytoplankton group. Given that there are no experimental constraints on DMS exudation rates, we assumed the lowest possible exudation rates that still allowed decoupling in the Tropics. Exudation of DMS by diatoms was set to be 10 times lower than the exudation rates of the other PFTs, according to what was found to be true for DMSP exudation (Archer et al., 2001). The exudation of DMSPd by phytoplankton has been neglected in this model. The exudation term is parameterised as

$$\left(\frac{\partial DMS}{\partial t}\right)_{exudation} = \lambda_{exud} * \frac{PAR}{PAR_{max}} * \text{DMSPp}, \tag{86}$$

where λ_{exud} is a constant rate term and PAR the incident solar radiation.

Cleavage of DMSP by free DMSP-lyase

A small fraction of the DMSPd is cleaved by free DMSP-lyase in the liquid phase (Scarratt et al., 2000). This DMSP-lyase is assumed to originate from DMSP-lyase containing algae and to have been released after cell lysis of those organisms. The cleavage by DMSP-lyase is a small and constant proportion (λ^{DL} of the DMSPd concentration.

$$\left(\frac{\partial DMSP}{\partial t}\right)_{cleavage} = -\lambda^{DL} * \text{DMSPd}. \tag{87}$$

9.1.4 Sink terms

Bacterial degradation of DMSPd

Bacterial degradation is described in Section 4.2.1. For DMSPd, equation 26 becomes:

$$L_{tot}^{bac} = \min(L_{nut}^{bac}, \frac{DMSPd}{DMSPd + K^{DMSPd}}) * bac_{limi}^{light} \tag{88}$$

where L_{nut}^{bac} is the bacterial nutrient limitation of the model, excluding DMSPd and bac_{limi}^{light} the bacterial limitation of DMSPd degradation as a function of insolation (Slezak et al., 2001).

Bacterial degradation of DMS

The formulation for bacterial degradation closely resembles the one used to simulate bacterial degradation of DMSPd. However, different half-saturation constants are used for both DMS and DMSPd (Archer et al., 2001). Hence,

$$\phi_{DMS}^{bac} = \mu^{bac} * L_{tot}^{bac} * f(T) * \alpha^{bac} * \text{BAC}, \tag{89}$$

where BAC and $f(T)$ are as above and

$$L_{tot}^{bac} = \min\left(L_{nut}^{bac}, \frac{DMS}{DMS + K_m^{DMS}}\right) * bac_{limi}^{light}. \tag{90}$$

Based on Vila-Costa et al., 2006, we assume that approximately 33% (α^{bac}) of the bacterial community can utilise DMS.

Photolysis of DMS

The photolysis rate for DMS is assumed to be a linear function of incident PAR and prevailing DMS concentration. In seawater, DMS is not directly photolysed (Brimblecombe and Shooter, 1986; Brugger et al., 1998), but oxidised by free radicals created through the photolysis of coloured dissolved organic matter (CDOM). Our formulation, however, does not take into account prevalent CDOM concentrations, as those are not modelled in PlankTOM5, due to the lack of world-wide evaluation data. The rate constants used are within the experimental range of uncertainty (Bailey et al., in press; Toole and Siegel, 2004) for the Sargasso Sea.

$$\left(\frac{\partial DMS}{\partial t}\right)_{photolysis} = -\lambda_{photo} * PAR * \text{DMS}, \tag{91}$$

where λ_{photo} is the rate coefficient for DMS photolysis.

9.1.5 Variable names

The evolution of DMS and DMSPd is calculated in the following Fortran routines:

- bgclos.F90 - production terms of DMS, DMSPd and computation of DMSPp
- bgcsnk.F90 - degradation of DMS and DMSPd
- bgcbio.F90 - recalculation of production terms after bgclos.F90 and bgcsnk.F90
- bgcnul.F90 - threshold value calculation for DMS and DMSPd
- bgcflx.F90 - sea-air transfer of DMS
- sms.F90 - initialisation of variables used in the sulphur cycle calculations
- trclsm.dgom.h90 - reads the sulphur cycle parameters from the namelist

The global variables used for the computation of the sulphur cycle are:

- prodms(jpi,jpj,jpk) - sum of all DMS production terms
- prodmd(jpi,jpj,jpk) - sum of all DMSPd production terms
- degdms(jpi,jpj,jpk) - sum of all DMS degradation terms
- degdmd(jpi,jpj,jpk) - sum of all DMSPd degradation terms
- trnbac(jpi,jpj,jpk) - proxy fuer bacterial biomass
- dmddms(jpi,jpj,jpk) - degradation terms for DMSPd that are source terms for DMS
- dmspp(jpi,jpj,jpk) - total intracellular DMSPp concentrations in mol L^{-1}

The global variables used for the computation of the sulphur cycle are:

- prodms(jpi,jpj,jpk) - sum of all DMS production terms
- prodmd(jpi,jpj,jpk) - sum of all DMSPd production terms
- degdms(jpi,jpj,jpk) - sum of all DMS degradation terms
- degdmd(jpi,jpj,jpk) - sum of all DMSPd degradation terms
- trnbac(jpi,jpj,jpk) - proxy fuer bacterial biomass
- dmddms(jpi,jpj,jpk) - degradation terms for DMSPd that are source terms for DMS
- dmspp(jpi,jpj,jpk) - total intracellular DMSPp concentrations in mol L^{-1}

9.1.6 Parameters for the DMS module of PlankTOM5

Table 18: List of Parameters used in evolution of DMS

Term	Variable	Description	Where set
α_{dms}	rn_rdddms	ratio of DMS/DMSP released by grazing	*namelist.trc.sms*
$q(i)_t$	rphdmd	DMSP/C cell ratio in phytoplankton	*bgclos.F90*
q_{min}	rn_rphdmd	DMSP/C mean cell ratio in phytoplankton	*namelist.trc.sms*
PAR_{max}	rn_etomax	maximum surface insolation	*namelist.trc.sms*
β^{mes}	rn_assdms	% of DMSP in meso fecal pellets lost	*namelist.trc.sms*
λ_{exud}	rn_xpldmd	DMSP leakage coefficient for phytoplankton	*namelist.trc.sms*
λ^{DL}	rn_xcldmd	DMSP-lyase DMSPd cleavage rate	*namelist.trc.sms*
μ^{bac}	rn_dmsyld	microbial yieald for DMS production	*namelist.trc.sms*
λ_{photo}	rn_xpodms	DMS photolysis rate coefficient	

Table 19: Parameters for the DMS module of PlankTOM5

Parameter	**Label**	**Value**	**Reference**
DMSPp cell quota:			
Diatoms	$\frac{S}{C}_{dia}$	0.002	Stefels et al. (2007)
Nanophytoplankton	$\frac{S}{C}_{dia}$	0.01	Stefels et al. (2007)
Coccolithophorids	$\frac{S}{C}_{dia}$	0.012	Stefels et al. (2007)
Ratio of Release DMS/DMSP in grazing by zooplankton	α_{dms}	0.1	Archer et al. (2001)
Fraction of DMSPp ingested that is released to the water colum:			
Proto-zooplankton grazing:	λ_i^{mic}	0.74	Buitenhuis et al. 2006
Meso-zooplankton grazing:	λ_i^{mes}	0.74	Buitenhuis et al. 2006
Fraction of DMSPd in fecal pellets lost in the grazing process:			
Proto-zooplankton	-	0%	Buitenhuis et al. (2006a)
Meso-zooplankton	-	50%	M. Steinke, pers comm.
DMS Exudation rates:			
Diatoms	λ_{exud}	0.005 d^{-1}	Archer et al. (2001)
Nanophtoplankton	λ_{exud}	0.05 d^{-1}	Archer et al. (2001)
Coccolithophorid	λ_{exud}	0.05 d^{-1}	Archer et al. (2001)
Fraction of DMSPd cleaved by free DMSP-lyase	λ^{DL}	0.01 d^{-1}	Archer et al. (2001)
Bacterial Temperature dependence		1.116	E. Buitenhuis, pers. comm.
Microbial yield DMSPd DMS conversion	μ^{bac}	0.1	Zubkov et al. (2001)
Bacterial Half-saturation constants			
DMSPd	Km_{DMSP}^{bac}	1.08 * 10^{-9}	Archer et al. (2001)
DMS	Km_{DMS}^{bac}	1.25 * 10^{-9}	Archer et al. (2001)
Photolysis rate	λ_{light}	0.05 d^{-1}	L.Bopp, pers. comm.
Maximal PAR	PAR_{max}	80 W m^{-2}	

Chapter 10

Air-sea exchange of trace gases

The air-sea flux of trace gases (CO_2, O_2, and DMS) is given by the product of gas exchange coefficient and the difference in concentration of the gas across the sea-air interface:

$$F_{air-sea} = k_w * (1 - \gamma) * (pC_{gas}^{air} - pC_{gas}^{sea}) \tag{92}$$

where k_w is the gas exchange coefficient, γ is the fraction of the ocean covered by ice, pC_{gas}^{air} is the concentration of the gas in the air directly above the water, and pC_{gas}^{sea} is the sea surface concentration of the gas.

The gas exchange coefficient is calculated according to Wanninkhof (1992) (eq. 3):

$$k_{wannin} = 0.3 * v^2 * \sqrt{660./Schmidt_{gas}} \tag{93}$$

where v is the amplitude of the winds (m/s), sst is the sea surface temperature, and Schmidt_{gas} is the Schmidt number for each gas Wanninkhof (1992).

10.1 CO_2

For the gas exchange coefficient CO_2 Wanninkhof (1992) include a chemical enhancement term:

$$k_{wannin}^{CO_2} = 0.3 * v^2 + 2.5 * (0.5246 + 0.016256 * sst + 0.00049946 * sst^2) \tag{94}$$

For CO_2, $pC_{CO_2}^{air}$ is calculated from the measured mixing ratio of CO_2 in the atmosphere ($C_{CO_2}^{air}$, in ppm) times the solubility of CO_2 in sea water and corrected for 100% water vapor Sarmiento et al. (1992):

$$pC_{CO_2}^{air} = C_{CO_2}^{air} * sol_{CO_2} * (1. - e^{20.1050 - 0.0097982 * sstk - 6163.10/sstk}) \tag{95}$$

where sstk is sea surface temperature in degree Kelvin. The solubility of CO_2 is given by:

$$sol_{CO_2} = e^{c00 + c01/(sstk*.01) + c02*\ln(sstk*.01) + sal*(c03 + c04*qtt + c05*(sstk*.01)^2)} * smicr \tag{96}$$

The Schmidt number for CO_2 is given by:

$$Schmidt_{CO_2} = 2073.1 - 125.62 * sst + 3.6276 * sst^2 - 0.043126 * sst^3 \tag{97}$$

where sal is the salinity and the coefficents $c00$, $c01$, $c02$, $c03$, $c04$, $c05$ and $smicr$ are given by Wanninkhof (1992).

$C_{CO_2}^{sea}$ is the concentration of CO_2 in the model, calculated based on the state variables DIC and TALK.

10.2 O_2

For O_2, $pC^{air}_{O_2}$ is calculated from the measured mixing ratio of O_2 in the atmosphere ($C^{air}_{O_2}$, times the solubility of O_2 in seawater, also corrected for 100% water vapor as for CO_2 Sarmiento et al. (1992):

$$pC^{air}_{O_2} = C^{air}_{O_2} * sol_{O_2} * (1. - e^{20.1050 - 0.0097982 * sstk - 6163.10/sstk}) \tag{98}$$

The solubility of O_2 is calculated as follows:

$$\begin{aligned} sol_{O_2} &= e^{ox0 + ox1/(sstk*.01) + ox2*\ln(sstk*.01) + sal*(ox3 + ox4*(sstk*.01) + ox5*(sstk*.01)^2)} \\ &* \quad oxyco \end{aligned} \tag{99}$$

The Schmidt number for O_2 is given by:

$$Schmidt_{O_2} = 1953.4 - 128.0 * sst + 3.9918 * sst^2 - 0.050091 * sst^3 \tag{100}$$

where sal is the salinity and the coefficents $ox0$, $ox1$, $ox2$, $ox3$, $ox4$, $ox5$, and $oxyco$ are given by Wanninkhof (1992).

10.3 DMS

Because the air concentration of DMS, C^{air}_{DMS}, is assumed to be negligeable the general flux equation is simplified to

$$F_{air} = k_w * DMS_{aq}, \tag{101}$$

The Schmitt number for DMS has been calculated according Saltzman et al. (1993).

$$Schmidt_c = 2674.0 - 147.12 * sst + 3.726 * sst^2 - 0.038 * sst^3 \tag{102}$$

Table 20: List of Parameters used in evolution of air-sea fluxes

Term	Variable	Description	Where set
v	vatm	wind speed	
sal	sn (1)	salinity of sea surface layer	
sst	tn (1)	temperature of sea surface (°C)	
$co1$	c00	and other chemical constants	*trcini.dgom.h90*
$Schmidt_{CO_2}$	schmico2	Schmidt number for CO_2	*bgcflx.F90*
$Schmidt_{O_2}$	schmio2	Schmidt number for O_2	*bgcflx.F90*
$Schmidt_{DMS}$	schmidms	Schmidt number for DMS	*bgcflx.F90*
γ	freeze	fraction of ocean covered by ice	*limflx.F90*

Chapter 11

Model Setup

11.1 Ocean General Circulation Model

The physical model NEMO v2.3 (Madec (2008),
http://www.nemo-ocean.eu/index.php//About-NEMO/Reference-manuals) was developed by the Laboratoire d' Océanographie Dynamique et de Climatologie (LODYC) to study large scale ocean circulation and its interaction with atmosphere and sea-ice. NEMO is based on the Navier-Stokes equations describing the motions of the fluid and on a non-linear equation of state, which couples the two tracers salinity and temperature to the fluid velocity.

11.2 Sea-Ice Model

NEMO is coupled to the Louvain-La-Neuve Sea-Ice Model (LIM, Timmermann et al., 2005), developed by Fichefet and Morales-Maqueda (1999). LIM has been thoroughly validated for both Arctic and Antarctic conditions, and has been used in a wide range of process studies. Due to the use of an elaborate technique for solving the continuity equations (Prather, 1986), LIM is particularly suited to describing the ice-edge in coarse grid resolutions, which are typically used for climate modelling studies. The physical fields that are advected in LIM are the ice concentration, the snow volume per unit area, the ice volume per unit area, the snow enthalpy per unit area, the ice enthalpy per unit area, and the brine reservoir per unit area. A full model description and details of the coupling to OPA-ORCA can be found in Timmermann et al. (2005).

11.3 Forcing

11.3.1 Physical Forcing

The model is forced by daily wind stress, cloud cover and precipitation from the NCEP/ NCAR reanalysed fields (Kalnay et al., 1996). Sensible and latent heat fluxes are calculated with bulk formulae using the differences between the surface temperature calculated by OPA and the observed air temperature, taking into account local humidity. At the end of each year a water balance is calculated and a uniform water flux correction is applied during the following year to conserve the water mass.

11.4 Initialisation

All model simulations are initialized with observations from the World Ocean Atlas 2005 for temperature (Locarnini et al., 2006), salinity (Antonov et al., 2006) PO_4^{3-},NO_3^-, SiO_3^-, (Garcia et al., 2006b) and O_2 (Garcia et al., 2006a). DIC, alkalinity (GLODAP) observations were from Key et al. (2004). $DI^{13}C$ is calculated according to Broecker and Peng (1982). The biological state variables are initialised with the output from previous model runs.

11.5 Dust input

The model is forced with Fe and Si input from monthly dust fluxes taken from Jickells et al. (2005) and interpolated to daily values in *bgcint.F90* . The input is total dust rather than in units of Fe. We assume 0.035g Fe per g of dust and either 8.8g Si per g Fe or, the equivalent, 0.308 g Si per g dust. The solubility of Fe in dust is generally taken to be 2 % and may be set in rn_fersol . The solubility of Si in dust is 7.5 %. Using these values the dust is converted to equivalent Fe and Si in units of mol/L/timestep in *trcini.dgom.h90* and *bgcbio.F90* .

In PlankTOM5 monthly dust fluxes from Tegen and Fung (1995) were used; in this case the input is in units of Fe.

11.6 River input

Annual fluxes of riverine carbon and nutrient (N, Si, Fe) to the ocean were computed following a global river drainage direction map (DDM30), considering population and basin area (Döll and Lehner, 2002), and river runoff (Kourzoun, 1977; Ludwig and Probst, 1998) at 0.5° increments of latitude and longitude as in da Cunha et al. (2007). This map represents the drainage directions of surface water on all continents, except Antarctica. Cells of the map are connected by their drainage directions and are thus organized into drainage basins. We use the cells corresponding to basin outlets to the ocean as input data for PlankTOM.

All riverine inputs may be switched off by setting the relevant parameter as listed in Table 21 to zero.

11.6.1 Dissolved Inorganic Nitrogen (DIN)

To calculate riverine DIN inputs we used a regression model originally developed by Smith et al. (2003):

$$\log DIN = 3.99 + 0.35 \log POP + 0.75 \log R \tag{103}$$

where (DIN) is in mol N km^{-2} y^{-1}, (POP) is population density in people km^{-2}, and (R) is runoff in m y^{-1}. The model describes DIN export by the analysis of 165 systems for which DIN flux data is available (Meybeck and A., 1997), S. Smith and F. Wulff (Eds.), LOICZ-Biogeochemical modelling node, 2000, available at http://data.ecology.su.se/MNODE/]. In this model, riverine DIN export to the coastal zone is a function of basin population density and runoff: On the basis of basin area, basin population (for the year 1990) and runoff provided by the DDM30 map, 16.3 Tg DIN y^{-1} (1.16 Tmol N y^{-1}) are transported to the coastal zone by rivers. In the Smith et al. 2003 model, the average N:P ratio of riverine export is 18:1, which is close to the PISCES-T N:P ratio of 16:1. Nitrogen retention in estuarine areas was not included owing to lack of global data.

11.6.2 Dissolved Silica (Si)

Rivers are responsible for 80% of the inputs of Si to the ocean (Treguer et al., 1995). For an estimate of riverine input of dissolved Si we used the runoff data from the DDM30 map, and applied an average concentration of Si in river waters of 4.2 mg Si/L (Treguer et al., 1995). Si concentration in river water is variable according to basin geology but regional data is not available. Our estimate leads to a dissolved Si river input of 187 Tg Si y^{-1} to the ocean. This value is comparable to the range of 140 30 Tg Si y^{-1} for a net riverine dissolved Si input to the ocean proposed by Treguer et al. (1995), considering estuarine retention of Si.

11.6.3 Dissolved Iron (Fe)

Rivers and continental shelf sediments supply Fe to surface waters. Because it is extensively removed from the dissolved phase in estuaries, rivers are thought to be a minor source for the open ocean, but not for coastal zones. We used the runoff data from the DDM30 map and applied an average concentration of dissolved Fe in river waters of 40 mg L^{-1} (Martin and Meybeck, 1979; Martin and Whitfield, 1983). As for Si, river basin geology influences Fe concentration in river water, but there is no available global database on riverine Fe. Our estimate leads to a gross dissolved Fe input of 1.75 Tg Fe y^{-1}, comparable to the estimate of 1.45 Tg Fe $^{-1}$ by Chester (1990). During estuarine mixing, flocculation of colloidal Fe and organic matter forms particulate Fe because of the major change in ionic strength upon mixing of fresh water and

seawater (de Baar and Jong, 2001). This removal has been well documented in many estuaries. Literature values show that approximately 80 to 99% of the gross dissolved Fe input is lost to the particulate phase in estuaries at low salinities (Boyle et al., 1977; Chester, 1990; Dai and Martin, 1995; Lohan and Bruland, 2006; Sholkovitz, 1978). We apply a removal rate of 99% to our gross Fe flux, and obtained a net input of riverine dissolved Fe to the coastal ocean of 0.02 Tg Fe y^{-1}.

11.6.4 Particulate (POC) and Dissolved Organic (DOC) and Inorganic (DIC) Carbon

The predicted river carbon fluxes are based on models relating river carbon fluxes to their major controlling factors (Ludwig and Probst, 1998; Ludwig, 1996). For POC, sediment flux is the dominant controlling parameter. For DOC, runoff intensity, basin slope, and the amount of soil OC in the basin are the controlling parameters (Ludwig, 1996). We applied this model to the DDM30 data set, and we estimate a gross discharge of 148 Tg C y^{-1} and 189 Tg C y^{-1} for POC and DOC, respectively. We assume that DOC has a conservative behavior in estuaries. These values are in agreement with recent modeled values of 170 Tg C y^{-1} as DOC (Harrison et al., 2005), and 197 Tg C y^{-1} as POC (Beusen et al., 2005; Seitzinger et al., 2005). We used a C:N:Fe ratio of 122:16:6.1 10^{-4}, thus riverine DOC and POC, when they are remineralized, are also N and Fe sources to the ocean. Inorganic carbon is mainly transported by rivers in the dissolved form. For DIC inputs, drainage intensity and river basin lithology are the controlling parameters (Ludwig et al., 1996). We applied this model to the DDM30 data set, and we estimate a DIC and alkalinity discharge of 385 Tg C y^{-1} (32.12 Tmol C y^{-1}).

11.7 The namelist.trc.sms file

Typical values for the parameters define in *namelist.trc.sms* are given in the following tables.

Table 21: List of Parameters used in river input

Term	Variable	Description	Where set
	rn_rivdic	river input of DIC	*namelist.trc.sms*
	rn_rivdoc	river input of DOC	*namelist.trc.sms*
	rn_rivpoc	river input of POC	*namelist.trc.sms*
	rn_rivnit	river input of nitrate	*namelist.trc.sms*
	rn_rivpo4	river input of phosphate	*namelist.trc.sms*
	rn_rivsil	river input of silica	*namelist.trc.sms*
	rn_sedfer	coastal release of Fe	*namelist.trc.sms*

Table 22: List of Parameters defined in *namelist.trc.sms* for PlankTOM10 (I)

Label	Value	Units	Description
rn_jpkbio	14	-	levels over which biology is calculated
rn_ag1poc	1.2e4	-	small POC (POC_s aggregation
rn_ag2poc	1e4	-	POC_s - large POC (POC_l) aggregation
rn_ag3poc	140	-	POC_s - POC_l aggregation
rn_ag4poc	150	-	POC_s aggregation
rn_ag5doc	180	-	DOC - POC_s aggregation
rn_ag6doc	3.9e3	-	DOC - POC_l aggregation
rn_coccal	0.433	-	ratio of $CaCO_3$ to organic carbon
rn_discal	0.75	-	fraction of $CaCO_3$ dissolved during coccolithophore mortality
rn_ekwgrn	0.0232	m^{-1}	green light absorption coefficient of H_2O
rn_ekwred	0.225	m^{-1}	red light absorption coefficient of H_2O
rn_faco18	0.98	-	bacterial fractionation for O_{18}
rn_fersol	0.02		
rn_gbadoc	0.9	-	relative preference of BAC grazing for DOC
rn_gbagoc	1.8	-	relative preference of BAC grazing for GOC
rn_gbapoc	1.8	-	relative preference of BAC grazing for POC
rn_ggebac	.374	-	growth efficiency BAC
rn_ggemac	0.29	-	growth efficiency MAC
rn_ggemes	0.26	-	growth efficiency MES
rn_ggemic	0.3	-	growth efficiency PRO
rn_ggtbac	0.0104		
rn_gmabac	0.000	-	relative preference of MAC grazing for BAC
rn_gmagoc	0.336	-	relative preference of MAC grazing for GOC
rn_gmames	2.016	-	relative preference of MAC grazing for MES
rn_gmamic	1.008	-	relative preference of MAC grazing for PRO
rn_gmapoc	0.336	-	relative preference of MES grazing for POC
rn_gmegoc	0.029	-	relative preference of MES grazing for GOC
rn_gmemic	2.882	-	relative preference of MES grazing for PRO
rn_gmepoc	0.29	-	relative preference of MES grazing for POC
rn_gmibac	2.374	-	relative preference of PRO grazing for BAC
rn_gmigoc	0.095	-	relative preference of PRO grazing for GOC
rn_gmipoc	0.095	-	relative preference of PRO grazing for POC
rn_gramac	0.2	d^{-1}	maximum MAC grazing rate
rn_grames	1.42	d^{-1}	maximum MES grazing rate
rn_gramic	1.27	d^{-1}	maximum PRO grazing rate
rn_grkmac	2.6e-7	mol L^{-1}	K_m for MAC grazing
rn_grkmes	2.6e-7	mol L^{-1}	K_m for MES grazing
rn_grkmic	6.5e-6	mol L^{-1}	K_m for PRO grazing
rn_grtmac	1.1079	-	temp. dependence of MAC grazing
rn_grtmes	1.059	-	temp. dependence of MES grazing
rn_grtmic	1.055	-	temp. dependence of PRO grazing
rn_kmfbac	0.025e-9	mol L^{-1}	K_m for Fe in DOC remineralisation by bacteria
rn_kmobac	5e-6	mol L^{-1}	K_m for DOC in DOC remineralisation by bacteria
rn_kmsbsi	20e-6		K_m for the Si/C ratio of diatoms
rn_lyscal	10e-5	mol L^{-1}	inertia conc. for $CaCO_3$ dissolution
rn_mokpft	1e-7	mol L^{-1}	K_m for zooplankton DOC exudation

Table 23: List of Parameters defined in *namelist.trc.sms* for PlankTOM10 (II)

Label	Value	Units	Description
rn_momphy	0.01	d^{-1}	phytoplankton minimum mortality rate
rn_mormac	0.015	d^{-1}	MAC mortality rate
rn_mormes	0.013	d^{-1}	MES mortality rate
rn_motmac	1.0654	-	temp. dependence of MAC mortality
rn_motmes	1.071	-	temp. dependence of MES mortality
rn_resbac	0.002	d^{-1}	BAC respiration at 0°C
rn_resmac	0.015	d^{-1}	MAC respiration at 0°C
rn_resmes	0.035	d^{-1}	MES respiration at 0°C
rn_resmic	0.004	d^{-1}	PRO respiration at 0°C
rn_resphy	0.00	d^{-1}	phytoplankton loss rate
rn_retbac	1.071	-	temp. dependence of BAC respiration
rn_retmac	1.1850	-	temp. dependence of MAC respiration
rn_retmes	1.1011	-	temp. dependence of MES respiration
rn_retmic	1.204	-	temp. dependence of PRO respiration
rn_rivdic	1.	mol $timestep^{-1}$	river input of DIC
rn_rivdoc	1.	mol $timestep^{-1}$	river input of DOC
rn_rivpoc	0.55	mol $timestep^{-1}$	river input of POC
rn_rivpo4	0.	mol $timestep^{-1}$	river input of PO_4
rn_rivsil	1.	mol $timestep^{-1}$	river input of silicate
rn_rivfer	0.05	mol $timestep^{-1}$	river input of FER
rn_scofer	0.01	$(mol\ L^{-1})^{-0.6}\ d^{-1}$	scavenging of Fe, f(POC_s, POC_l)
rn_sedfer	5e-11	mol L^{-1}	coastal release of Fe
rn_sigmac	0.70	-	fraction of MAC excretion as PO_4
rn_sigmes	0.68	-	fraction of MES excretion as PO_4
rn_sigmic	0.66	-	fraction of PRO excretion as DOM
rn_sildia	.42e-6	mol L^{-1}	$K_m^{SiO_3}$ for diatoms
rn_singoc	24000.0	-	parameters for sinking rate of POC_l, $CaCO_3$ and DSi
rn_snkgoc	20.0	m d^{-1}	parameter for sinking speed of POC_l,$CaCO_3$ and SiO_2
rn_snkpoc	3.0	m d^{-1}	sinking speed of POC_s
rn_unamac	0.18	-	unassimilated fraction of phyto during MAC grazing
rn_unames	0.3	-	unassimilated fraction of phyto during MES grazing
rn_unamic	0.1	-	unassimilated fraction of phyto during PRO grazing
rn_docphy	0.05	d^{-1}	phytoplankton excretion rate: DIA
	0.05		phytoplankton excretion rate: MIX
	0.05		phytoplankton excretion rate: COC
	0.05		phytoplankton excretion rate: PIC
	0.05		phytoplankton excretion rate: PHA
	0.05		phytoplankton excretion rate: FIX

Table 24: List of Parameters defined in *namelist.trc.sms* for PlankTOM10 (III)

Label	Value	Units	Description
rn_gmaphy	1.008		relative preference of MAC for DIA
	1.008		relative preference of MAC for MIX
	1.008		relative preference of MAC for COC
	.336		relative preference of MAC for PIC
	.672		relative preference of MAC for PHA
	.336		relative preference of MAC for FIX
rn_gmephy	2.882		relative preference of MES for DIA
	1.441		relative preference of MES for MIX
	1.441		relative preference of MES for COC
	0.000		relative preference of MES for PIC
	0.095		relative preference of MES for PHA
	0.000		relative preference of MES for FIX
rn_gmiphy	0.142		relative preference of MIC for DIA
	0.237		relative preference of MIC for MIX
	0.237		relative preference of MIC for COC
	0.95		relative preference of MIC for PIC
	0.142		relative preference of MIC for PHA
	0.010		relative preference of MIC for FIX
rn_kmfphy	.10e-9	mol L^{-1}	K_m^{Fe} for DIA
	.04e-9	mol L^{-1}	K_m^{Fe} for MIX
	.04e-9	mol L^{-1}	K_m^{Fe} for COC
	.04e-9	mol L^{-1}	K_m^{Fe} for PIC
	.06e-9	mol L^{-1}	K_m^{Fe} for PHA
	.15e-9	mol L^{-1}	K_m^{Fe} for FIX
rn_kmnphy	.53e-6	mol L^{-1}	K_m^{N} for DIA
	.80e-6	mol L^{-1}	K_m^{N} for MIX
	.060e-6	mol L^{-1}	K_m^{N} for COC
	0.39e-6	mol L^{-1}	K_m^{N} for DIA
	4.0e-6	mol L^{-1}	K_m^{N} for MIX
	13.e-6	mol L^{-1}	K_m^{N} for COC
rn_kmpphy	6.5e-6	mol L^{-1}	$K_m^{PO_4}$ for DIA
	6.1e-6	mol L^{-1}	$K_m^{PO_4}$ for MIX
	.460e-6	mol L^{-1}	$K_m^{PO_4}$ for COC
	1.2e-6	mol L^{-1}	$K_m^{PO_4}$ for PIC
	300.0e-6	mol L^{-1}	$K_m^{PO_4}$ for PHA
	0.00095e-5	mol L^{-1}	$K_m^{PO_4}$ for FIX
rn_morphy	0.0	d^{-1}	maximum mortality DIA (not used)
	0.0	d^{-1}	maximum mortality MIX (not used)
	0.0	d^{-1}	maximum mortality COC (not used)
	0.0	d^{-1}	maximum mortality PIC (not used)
	0.0	d^{-1}	maximum mortality PHA (not used)
	0.0	d^{-1}	maximum mortality FIX (not used)
rn_mulphy	4.0	-	dependence of PI slope on light intensity DIA
	7.0	-	dependence of PI slope on light intensity MIX
	6.0	-	dependence of PI slope on light intensity COC
	11.0	-	dependence of PI slope on light intensity PIC
	6.0	-	dependence of PI slope on light intensity PHA
	3.0	-	dependence of PI slope on light intensity FIX

Table 25: List of Parameters defined in *namelist.trc.sms* for PlankTOM10 (IV)

Label	Value	Units	Description
rn_mumpft	0.80	d^{-1}	maximum growth rate DIA
	0.63	d^{-1}	maximum growth rate MIX
	0.19	d^{-1}	maximum growth rate COC
	0.15	d^{-1}	maximum growth rate PIC
	0.90	d^{-1}	maximum growth rate PHA
	0.04	d^{-1}	maximum growth rate FIX
	2.45	d^{-1}	maximum growth rate BAC
rn_mdtpft	22.5	d^{-1}	maximum growth rate PRO
	33.0	d^{-1}	maximum growth rate MES
	30.0	d^{-1}	maximum growth rate MAC
	21.4	d^{-1}	maximum growth rate DIA
	28.0	d^{-1}	maximum growth rate MIX
	20.2	d^{-1}	maximum growth rate COC
	23.5	d^{-1}	maximum growth rate PIC
	22.4	d^{-1}	maximum growth rate PHA
	28.5	d^{-1}	maximum growth rate FIX
	21.2	d^{-1}	maximum growth rate BAC
rn_mupphy	0.0	-	penalty for DIA growth if MLD $>$ 2* euphotic depth
	0.2	-	penalty for MIX growth if MLD $>$ 2* euphotic depth
	0.3	-	penalty for COC growth if MLD $>$ 2* euphotic depth
	0.0	-	penalty for PIC growth if MLD $>$ 2* euphotic depth
	0.3	-	penalty for PHA growth if MLD $>$ 2* euphotic depth
	0.4	-	penalty for FIX growth if MLD $>$ 2* euphotic depth
rn_mutpft	1.040	-	temp. dependence of proto-zooplankton
	1.0718	-	temp. dependence of meso-zooplankton
	1.1443	-	temp. dependence of macro-zooplankton
	1.0744	-	temp. dependence of DIA
	1.0461	-	temp. dependence of MIX
	1.1325	-	temp. dependence of COC
	1.1169	-	temp. dependence of PIC
	1.0520	-	temp. dependence of PHA
	1.1142	-	temp. dependence of FIX
	1.0588	-	temp. dependence of BAC

Chapter 12

Output

The following files are output during a PlankTOM run for a simulation named *NAME* for year *nnnn*:

ocean.output.*nnnn*

date.num

EMPave_*nnnn*.dat

restart_*nnnn*1231_opa.nc

restart_*nnnn*1231_trc.nc

restart_*nnnn*1231_ice.nc

*NAME*_*nnnn*_gridT.nc

*NAME*_*nnnn*_gridU.nc

*NAME*_*nnnn*_gridV.nc

*NAME*_*nnnn*_gridW.nc

*NAME*_*nnnn*_diad.nc

*NAME*_*nnnn*_ptrc.nc

The file ocean.output.*nnnn* is written during the run and provides a log of the input used and the progress of the run. The next five files (EMPave_*nnnn*.dat, date.num, restart_*nnnn*1231_opa.nc, restart_*nnnn*1231_trc.nc, restart_*nnnn*1231_ice.nc) are required before PlankTOM can be run for the following year. date.num contains the last day of the run e.g. 19481231) EMPave_*nnnn*.dat contains the freshwater budget correction. The grid files contain output from the physical model and are not described in detail here.

The fields contained in the file *NAME*_*nnnn*_diad.nc (after the longitude, latitude, depth and time information) are described in Table 26 and the fields contained in the file *NAME*_*nnnn*_ptrc.nc are described in Table 27.

Table 26: Fields in the file *NAME_nnnn*_diad.nc

Field	Dimension	Description	Units
EXP	4	export	mol/m2/s
GRAMAC	4	Total macro-zooplankton grazing	mol/m3/s
GRAMIC	4	Total proto-zooplankton grazing	mol/m3/s
PPT	4	Primary production	molC/m3/s
GRAMICPHY	4	Proto-zooplankton grazing on phytoplankton	molC/m3/s
GRAMESPHY	4	Meso-zooplankton grazing on phytoplankton	molC/m3/s
GRAMES	4	Total meso-zooplankton grazing	mol/m3/s
GRAMACPHY	4	Macro-zooplankton grazing on phytoplankton	molC/m3/s
denitr	4	Denitrification	molN/m3/s
DEL02	4	Oxygen consumption	mol/m3/s
nitrfix	4	Nitrogen fixation	molN/m3/s
		The following fields are calculated at the surface	
respz	3	DIC exudation by proto-zooplankton	mol/m3/s
tortz	3	Proto-zooplankton mortality	mol/m3/s
grapoc	3	POC production by proto-zooplankton feeding and phytoplankton mortality	
grarem	3	Reminerlaisation due to proto-zooplankton grazing	
gramit	3	Total proto-zooplankton grazing	mol/m3/s
gramicphy	3	Proto-zooplankton grazing on phytoplankton	mol/m3/s
grabac	3	Proto-zooplankton grazing on bacteria	mol/m3/s
grazm	3	Proto-zooplankton grazing on POC	mol/m3/s
respz2	3	DIC exudation by meso-zooplankton	mol/m3/s
tortz2	3	Meso-zooplankton mortality	mol/m3/s
grapoc2	3	POC production by meso-zooplankton feeding	mol/m3/s
grarem2	3	Remineralisation due to meso-zooplankton grazing	mol/m3/s
gramet	3	Total meso-zooplankton grazing	mol/m3/s
gramesphy	3	Meso-zooplankton grazing on phytoplankton	mol/m3/s
grazoc	3	Meso-zooplankton grazing on POC and GOC	mol/m3/s
Cflx	3		mol/m2/s
grazz	3	Meso-zooplankton grazing on proto-zooplankton	mol/m3/d
respz3	3	DIC exudation by macro-zooplankton	mol/m3/d
tortz3	3	Macro-zooplankton mortality	mol/m3/s
grapoc3	3	GOC production by macro-zooplankton feeding	mol/m3/s
grarem3	3	Remineralisation due to macro-zooplankton grazing	mol/m3/s
gramat	3	Total macro-zooplankton grazing	mol/m3/s
gramacphy	3	Macro-zooplankton grazing on phytoplankton	mol/m3/s
grampoc	3	Macro-zooplankton grazing on POC	mol/m3/s
gramgoc	3	Macro-zooplankton grazing on GOC	mol/m3/s
gramaczoo	3	Macro-zooplankton grazing on micro- and meso-zooplankton	mol/m3/s
Oflx	3		mol/m2/s
DpCO2	3		ppm

Table 27: Fields in the file *NAME_nnnn*_ptrc.nc

Field	Dimension	Description	Units
Alkalini	4	Alkalinity concentration	eq/L
O2	4	Oxygen concentration	mol/L
CaCO3	4	Calcite concentration	mol/L
DOC	4	DOC concentration	mol/L
POC	4	POC concentration	mol/L
GOC	4	Big POC concentration	mol/L
SFe	4	Small Fe particles concentration	mol/L
BFe	4	Big Fe particles concentration	mol/L
DSi	4	Particulate Si concentration	mol/L
DIC	4	DIC concentration	mol/L
NO3	4	DIN concentration	mol/L
PO4	4	Phosphate concentratio	mol C/L
Fer	4	Iron concentration	mol/L
Si	4	Silicate concentration	mol/L
PRO	4	Proto-zooplankton concentration	mol/L
MES	4	Meso-zooplankton concentration	mol/L
MAC	4	Macro-zooplankton concentration	mol/L
DIA	4	Diatoms concentration	mol/L
MIX	4	Mixed phytoplankton concentration	mol/L
COC	4	Coccolithophorid concentration	mol/L
PIC	4	Picophytoplankton concentration	mol/L
PHA	4	Phaeocystis concentration	mol/L
FIX	4	N2-fixers concentration	mol/L
DFe	4	Diatoms Fe concentration	mol/L
Nfe	4	Mixed phytoplankton Fe concentration	mol/L
CFe	4	Coccolithophorid Fe concentration	mol/L
PFe	4	Picophytoplankton Feconcentration	mol/L
HFe	4	Phaeocystis Fe concentration	mol/L
FFe	4	N2-fixers Fe concentration	mol/L
DCHL	4	Diatoms chlorophyll concentration	mol/L
NCHL	4	Mixed phytoplankton chlorophyll concentration	mol/L
CCHL	4	Coccolithophorid chlorophyll concentration	mol/L
PCHL	4	Picophytoplankton chlorophyll concentration	mol/L
HCHL	4	Phaeocystis chlorophyll concentration	mol/L
FCHL	4	N2-fixers chlorophyl concentration	mol/L
BSi	4	Diatoms Si concentration	mol/L
BAC	4	Bacteria concentration	mol/L

Bibliography

Alldredge, A. L. and Gotschalk, C. (1988). In situ settling behaviour of marine snow. *Limnol. Oceanogr.*, 33:339–351.

André, J. M. (1990). *Télédétection spaciale de la couleir de la mer: algorithme d' inversion des mesures du Coastal Zone Color Scanner. Application à l' étude de la Méditerranée occidentale*. PhD thesis, Université Pierre et Marie Curie Paris VI, France.

Antonov, J. I., Locarnini, R., Boyer, T., Mishonov, A., and Garcia, H. (2006). *World Ocean Atlas 2005, Volume 2: Salinity.* S. Levitus, Ed. NOAA Atlas NESDIS 62, U.S. Government Printing Office, Washington, D.C.

Archer, S. D., Widdicombe, C. E., Tarran, G. A., Rees, A. P., and Burkill, P. H. (2001). Production and turnover of particulate dimethylsulphoniopropionate during a coccolithophore bloom in the northern North Sea. *Aquatic Microbial Ecology*, 24(3):225–241.

Aumont, O. and Bopp, L. (2006a). Globalizing results from ocean in situ fe fertilisation studies. *Global Biogeochemical Cycles*, 20:doi:10.1029/2005GB002591.

Aumont, O. and Bopp, L. (2006b). Globalizing results from ocean in situ iron fertilization studies. *Global Biogeochemical Cycles*, 20:GB2017, doi:10.1029/2005GB002591.

Aumont, O., Maier-Reimer, E., Blain, S., and Monfray, P. (2003). An ecosystem model of the global ocean including Fe, Si, P colimitations. *Global Biogeochemical Cycles*, 17(2):1060, doi:10.1029/2001GB001745.

Beusen, A., Dekkers, A., Bouwman, A., Ludwig, W., and Harrison, J. (2005). Estimation of global river transport of sediments and associated particulate C, N, and P. *Global Biogeochemical Cycles*, 19(4).

Boyle, E., Edmond, J., and Sholkovitz, E. (1977). Mechanism of iron removal in estuaries. *Geochimica et Cosmochimica Acta*, 41(9):1313–1324.

Brimblecombe, P. and Shooter, D. (1986). Photooxidation of dimethylsulfide in aqueous-solution. *Marine Chemistry*, 19(4):343–353.

Broecker, W. and Peng, T. H. (1982). *Tracers in the sea*. Eldigio Press Lamont Doherty Geological Observatory.

Brugger, A., Slezak, D., Obernosterer, I., and Herndl, G. J. (1998). Photolysis of dimethylsulfide in the northern Adriatic Sea: Dependence on substrate concentration, irradiance and doc concentration. *Marine Chemistry*, 59(3-4):321–331.

Buitenhuis, E., Le Quere, C., Aumont, O., Beaugrand, G., Bunker, A., Hirst, A., Ikeda, T., O'Brien, T., Piontkovski, S., and Straile, D. (2006a). Biogeochemical fluxes through mesozooplankton. *Global Biogeochemical Cycles*, 20:GB2003, doi:10.1029/2005GB002511.

Buitenhuis, E., Le Quéré, C., Aumont, O., Beaugrand, G., Bunker, A., Hirst, A., Ikeda, T., O'Brien, T., Piontkovski, S., and Straile, D. (2006b). Biogeochemical fluxes through mesozooplankton. *Global Biogeochemical Cycles*, 20:GB2003, doi:10.1029/2005GB002511.

Buitenhuis, E., van der Wal, P., and de Baar, H. J. (2001). Blooms of emiliana huxleyi are sinks of atmospheric carbon dioxide: a field and mesocosm study derived simulation. *Global Biogeochemical Cycles*, 15:577–587.

Buitenhuis, E. T., Pangerc, T., Franklin, D. J., Le Quéré, C., and Malin, G. (2008). Growth rates of six coccolithophorid strains as a function of temperature. *Limnol. Oceanogr*, 53(3):1181–1185.

Chester, R. (1990). *Marine Geochemistry*. Unwin Hyman.

da Cunha, L., Buitenhuis, E. T., Le Quéré, C., Giraud, X., and Ludwig, W. (2007). Potential impact of changes in river nutrient supply on global ocean biogeochemistry. *Global Biogeochemical Cycles*, 21:GB4007, doi:10.1029/2006GB002718.

Dai, M. and Martin, J. (1995). First data on trace-metal level and behavior in 2 major arctic river-estuarine systems (ob and yenisey) and in the adjacent kara sea, russia. *Earth And Planetary Science Letters*, 131(3-4):127–141.

de Baar, H. J. W. and Jong, J. T. M. D. (2001). Distributions, sources and sinks of iron in seawater. In Turner, D. R. and Hunter, K. A., editors, *The Biogeochemistry of Iron in Seawater*, pages 123–153. John Wiley.

Döll, P. and Lehner, B. (2002). Validation of a new global 30-min drainage direction map. *Journal Of Hydrology*, 258(1-4):214–231.

Fichefet, T. and Morales-Maqueda, M. A. (1999). Modelling the influence of snow accumulation and snow-ice formation on the seasonal cycle of the Antarctic sea-ice cover. *Climate Dynamics*, 15(4):251–268.

Garcia, H., Locarnini, R., Boyer, T., and Antonov, J. I. (2006a). *World Ocean Atlas 2005, Volume 3: Dissolved Oxygen, Apparent Oxygen Utilization, and Oxygen Saturation*. S. Levitus, Ed. NOAA Atlas NESDIS 63, U.S. Government Printing Office, Washington, D.C.

Garcia, H., Locarnini, R., Boyer, T., and Antonov, J. I. (2006b). *World Ocean Atlas 2005, Volume 4: Nutrients (phosphate, nitrate, silicate)*. S. Levitus, Ed. NOAA Atlas NESDIS 64, U.S. Government Printing Office, Washington, D.C.

Geider, R. J., MacIntyre, H. L., and Kana, T. D. (1996). A dynamic model of photoadaptation in phytoplankton. *Limnology and Oceanography*, 41:1–15.

Geider, R. J., MacIntyre, H. L., and Kana, T. D. (1998). A dynamic regulatory model of phytoplanktonic acclimation to light, nutrients and temperature. *Limnology and Oceanography*, 43:679–694.

Harrison, J., Caraco, N., and Seitzinger, S. (2005). Global patterns and sources of dissolved organic matter export to the coastal zone: Results from a spatially explicit, global model. *Global Biogeochemical Cycles*, 19(4).

IPCC (2007). *Climate Change 2007: The Physical Science Basis: Contribution of Working Group I to the Fourth Assessment Report of the International Panel on Climate Change*. Cambridge University Press, Cambridge, United Kingdom and New York, NY, USA, 1 edition.

Jickells, T. D., An, Z. S., Andersen, K. K., Baker, A. R., Bergametti, G., Brooks, N., Cao, J. J., Boyd, P. W., Duce, R. A., Hunter, K. A., Kawahata, H., Kubilay, N., laRoche, J., Liss, P., Mahowald, N., Prospero, J. M., Ridgwell, A. J., Tegen, I., and Torres, R. (2005). Global iron connections betwen desert dust, ocean biogechemistry, and climate. *Science*, 308:67–71.

Kalnay, E., Kanamitsu, M., Kistler, R., Collins, W., Deaven, D., Gandin, L., Iredell, M., Saha, S., White, G., Woollen, J., Zhu, Y., Chelliah, M., Ebisuzaki, W., Higgins, W., Janowiak, J., Mo, K. C., Ropelewski, C., Wang, J., Leetmaa, A., Reynolds, R., Jenne, R., and Joseph, D. (1996). The NCEP/NCAR 40-year reanalysis project. *Bulletin of the American Meteorological Society*, 77(3):437–471.

Karsten, U., Kuck, K., Vogt, C., and Kirst, G. O. (1996). Dimethylsulfoniopropionate production in phototrophic organisms and its physiological function as a cryoprotectant. *Biological and Environmental Chemistry of Dmsp and Related Sulfonium Compounds*, pages 143–153.

Karsten, U., Wiencke, C., and Kirst, G. O. (1992). Dimethylsulphoniopropionate (DMSP) accumulation in green macroalgae from polar to temperate regions - interactive effects of light versus salinity and light versus temperature. *Polar Biology*, 12(6-7):603–607.

Key, R., Kozyr, A., Sabine, C., Lee, K., Wanninkhof, R., Bullister, J., Feely, R., Millero, F., Mordy, C., and Peng, T.-H. (2004). A global ocean carbon climatology: Results from glodap. *Global Biogeochemical Cycles*, 18(GB4031).

Kourzoun, V. I. (1977). *Atlas of World Water Balance*. UNESCO.

Le Quéré, C., Harrison, S. P., Prentice, I. C., Buitenhuis, E. T., Aumont, O., Bopp, L., Claustre, H., Cotrim da Cunha, L., Geider, R., Giraud, X., Klaas, C., Kohfeld, K., Legendre, L., Manizza, M., Platt, T., Rivkin, R. B., Sathyendranath, S., Uitz, J., Watson, A. J., and Wolf-Gladrow, D. (2005). Ecosystem dynamics based on plankton functional types for global ocean biogeochemistry models. *Global Change Biology*, 11(11):2016–2040.

Locarnini, R. A., A.V., M., J.I., A., T.P., B., and H.E., G. (2006). *World Ocean Atlas 2005, Volume 1: Temperature.* S. Levitus, Ed. NOAA Atlas NESDIS 61, U.S. Government Printing Office, Washington, D.C.

Lohan, M. and Bruland, K. (2006). Importance of vertical mixing for additional sources of nitrate and iron to surface waters of the Columbia River plume: Implications for biology. *Marine Chemistry*, 98(2-4):260–273.

Ludwig, W., e. a. (1996). River discharges of carbon to the world's oceans: Determining local inputs of alkalinity and of dissolved and particulate organic carbon. *Comptes Rendus de l'Academie des Sciences - Serie IIA Sci. Terres Planetes*, 323(12):1007–1014.

Ludwig, W., Probst, J., and Kempe, S. (1996). Predicting the oceanic input of organic carbon by continental erosion. *Global Biogeochemical Cycles*, 10(1):23–41.

Ludwig, W. and Probst, J. L. (1998). River sediment discharge to the oceans: Present-day controls and global budgets. *American Journal of Science*, 298:265–295.

Madec, G. (2008). *NEMO ocean engine Note du pole de modélisation*, volume 27. Institut Pierre-Simon Laplace, Paris.

Maier-Reimer, E. (1993). Geochemical cycles in an ocean general circulation model: Preindustrial reacer distributions. *Global Biogeochem. Cycles.*, 7:645–677.

Martin, J.-M. and Meybeck, M. (1979). Elemental mass-balance of material carried by major world rivers. *Marine Chemistry*, 7(3):173–206.

Martin, J.-M. and Whitfield, M. (1983). The significance of the river input of chemical elements to the ocean. In Wong, C., Boyle, E., Bruland, K., and Burton, J.D.and Goldberg, E., editors, *Trace Metals in Sea Water*, pages 265–296. Plenum.

Meybeck, M. and A., R. (1997). River discharges to the oceans: An assessment of suspended solids, major ions, and nutrients. Technical report, U.N. Environ. Programme.

Prather, M. C. (1986). Numerical advection by conservation of second-order moments. *Journal of Geophysical Research*, 91(D6):6671–6681.

Saltzman, E. S., King, D. B., Holmen, K., and Leck, C. (1993). Experimental-determination of the diffusion-coefficient of dimethylsulfide in water. *Journal of Geophysical Research-Oceans*, 98(C9):16481–16486.

Sarmiento, J. L., Orr, J. C., and Siegenthaler, U. (1992). A perturbation simulation of CO_2 uptake in an ocean general-circulation model. *Journal of Geophysical Research-Oceans*, 97(C3):3621–3645.

Sarthou, G., Timmermans, K. R., Blain, S., and Tréguer, P. (2005). Growth physiology and fate of diatoms in the oceans: a review. *Joural of Sea Research*, 53:25–42.

Scarratt, M., Cantin, G., Levasseur, M., and Michaud, S. (2000). Particle size-fractionated kinetics of DMS production: where does DMSP cleavage occur at the microscale? *Journal of Sea Research*, 43(3-4):245–252.

Seitzinger, S., Harrison, J., Dumont, E., Beusen, A., and Bouwman, A. (2005). Sources and delivery of carbon, nitrogen, and phosphorus to the coastal zone: An overview of global nutrient export from watersheds (news) models and their application. *Global Biogeochemical Cycles*, 19(4).

Sholkovitz, E. (1978). Flocculation of dissolved fe, mn, al, cu, ni, co and cd during estuarine mixing. *Earth And Planetary Science Letters*, 41(1):77–86.

Slezak, D., Brugger, A., and Herndl, G. J. (2001). Impact of solar radiation on the biological removal of dimethylsulfoniopropionate and dimethylsulfide in marine surface waters. *Aquatic Microbial Ecology*, 25(1):87–97.

Smith, S., Swaney, D., Talaue-McManus, L., Bartley, J., Sandhei, P., McLaughlin, C., Dupra, V., Crossland, C., Buddemeier, R., Maxwell, B., and Wulff, F. (2003). Humans, hydrology, and the distribution of inorganic nutrient loading to the ocean. *Bioscience*, 53(3):235–245.

Stefels, J., Steinke, M., Turner, S., Malin, G., and Belviso, S. (2007). Environmental constraints on the production and removal of the climatically active gas dimethylsulphide (DMS) and implications for ecosystem modelling. *Biogeochemistry*, 83(1-3):245–275.

Sunda, W., Kieber, D. J., Kiene, R. P., and Huntsman, S. (2002). An antioxidant function for DMSP and DMS in marine algae. *Nature*, 418(6895):317–320.

Tegen, I. and Fung, I. (1995). Contribution to the atmospheric mineral aerosol load from land-surface modification. *Journal of Geophysical Research-Atmospheres*, 100(D9):18707–18726.

Timmermann, R., Goosse, H., Madec, G., Fichefet, T., Ethe, C., and Duliere, V. (2005). On the representation of high latitude processes in the ORCA-LIM global coupled sea ice-ocean model. *Ocean Modelling*, 8(1-2):175–201.

Toole, D. A. and Siegel, D. A. (2004). Light-driven cycling of dimethylsulfide (DMS) in the Sargasso Sea: Closing the loop. *Geophysical Research Letters*, 31:L09308, doi:10.1029/2004GL019581.

Treguer, P., Nelson, D., Vanbennekom, A., Demaster, D., Leynaert, A., and Queguiner, B. (1995). The silica balance in the world ocean - a reestimate. *Science*, 268(5209):375–379.

Vallina, S. M., Simó, R., Anderson, T. R., Gabric, A., Cropp, R., and Pacheco, J. M. (2008). A dynamic model of oceanic sulfur (DMOS) applied to the Sargasso Sea: Simulating the dimethylsulfide (DMS) summer paradox. *Journal of Geophysical Research-Biogeosciences*, 113:G01009, doi:10.1029/2007JG000415.

Vila-Costa, M., del Valle, D. A., Gonzalez, J. M., Slezak, D., Kiene, R. P., Sanchez, O., and Simó, R. (2006). Phylogenetic identification and metabolism of marine dimethylsulfide-consuming bacteria. *Environmental Microbiology*, 8(12):2189–2200.

Wanninkhof, R. (1992). Relationship between wind-speed and gas-exchange over the ocean. *Journal of Geophysical Research-Oceans*, 97(C5):7373–7382.

Wolf-Gladrow, D. A., Zeebe, R. E., Klaas, C., Koertzinger, A., and Dickson, A. (2007). Total alkalinity: the explicit conservative expression and its application to biogeochmical processes. *Marine chemistry*, 106:287–300.

Zubkov, M. V., Fuchs, B. M., Archer, S. D., Kiene, R. P., Amann, R., and Burkill, P. H. (2001). Linking the composition of bacterioplankton to rapid turnover of dissolved dimethylsulphoniopropionate in an algal bloom in the north sea. *Environmental Microbiology*, 3(5):304–311.

Index